

Variable Time-Fraction Collaborative Communications

Patrick Tooher

A Thesis in the
Department of Electrical and Computer Engineering

Presented in Partial Fulfillment of the Requirements
For the Degree of Doctor of Philosophy at
Concordia University
Montreal, Quebec, Canada

September 2009

© Patrick Tooher, 2009



Library and Archives
Canada

Published Heritage
Branch

395 Wellington Street
Ottawa ON K1A 0N4
Canada

Bibliothèque et
Archives Canada

Direction du
Patrimoine de l'édition

395, rue Wellington
Ottawa ON K1A 0N4
Canada

Your file *Votre référence*
ISBN: 978-0-494-67373-7
Our file *Notre référence*
ISBN: 978-0-494-67373-7

NOTICE:

The author has granted a non-exclusive license allowing Library and Archives Canada to reproduce, publish, archive, preserve, conserve, communicate to the public by telecommunication or on the Internet, loan, distribute and sell theses worldwide, for commercial or non-commercial purposes, in microform, paper, electronic and/or any other formats.

The author retains copyright ownership and moral rights in this thesis. Neither the thesis nor substantial extracts from it may be printed or otherwise reproduced without the author's permission.

AVIS:

L'auteur a accordé une licence non exclusive permettant à la Bibliothèque et Archives Canada de reproduire, publier, archiver, sauvegarder, conserver, transmettre au public par télécommunication ou par l'Internet, prêter, distribuer et vendre des thèses partout dans le monde, à des fins commerciales ou autres, sur support microforme, papier, électronique et/ou autres formats.

L'auteur conserve la propriété du droit d'auteur et des droits moraux qui protègent cette thèse. Ni la thèse ni des extraits substantiels de celle-ci ne doivent être imprimés ou autrement reproduits sans son autorisation.

In compliance with the Canadian Privacy Act some supporting forms may have been removed from this thesis.

While these forms may be included in the document page count, their removal does not represent any loss of content from the thesis.

Conformément à la loi canadienne sur la protection de la vie privée, quelques formulaires secondaires ont été enlevés de cette thèse.

Bien que ces formulaires aient inclus dans la pagination, il n'y aura aucun contenu manquant.


Canada

ABSTRACT

Variable Time-Fraction Collaborative Communications

Patrick Tooher, Ph.D.

Concordia University 2009

In order to improve the performance of the wireless channel, collaborative communications has recently been proposed. In such a scenario, a source wishing to transmit a signal to a destination can be aided by an otherwise idle transmitter (labeled a relay). Due to the half duplex constraint, the relay node cannot transmit and receive at the same time. It has been shown that having a variable amount of time for which the relay will receive data, can provide further gains in collaborative communications. In this thesis we develop and study methods to implement the use of a variable time-fraction in collaborative communications. We study our proposed method under different channel state information scenarios.

We design channel codes that allow for a relay to collaborate with a finite set of time-fractions. Through analysis, we provide design criteria that allow variable time-fraction collaborative codes to optimize their error rate performance. Our variable time-fraction collaborative codes are shown to approach the outage probability of collaborative channels. Furthermore, through the use of an upper bound on the error rate, we show the robustness of variable time-fraction collaboration over all relay locations when compared to traditional fixed time-fraction collaboration.

Next we study the effect of imperfect channel state information at the receivers. It is shown that the effect of estimation errors is twofold in collaborative communications. Firstly the relay will have diminished collaborative capabilities and secondly, the destination suffers performance degradation.

Assuming full and perfect channel state information at the transmitters, we design and study the use of power allocation algorithms (*PAA*). Our proposed optimal *PAA* (*OPAA*) optimizes the error rate performance of variable time-fraction collaborative communications. We also provide a more robust suboptimal *PAA* (*SPAA*) whose results suffer slight degradation compared to the *OPAA*.

Lastly, we study the effect of imperfect channel state information at both the transmitters and the receivers. Our analysis shows the independence of the optimal number of pilot symbols to the location of the relay.

To my late parents, who have always been there for me.

Acknowledgements

First I would like to express my gratitude to my thesis supervisor Dr. M. Reza Soleymani. Through his support and guidance I have been able to learn much more than what can be contained in a thesis. Dr. Soleymani understands that the value of the learning process is at least equal to that of the end result. His timely advice as well as words of encouragement allowed me to extract as much as possible from my experiences as a graduate student.

I would like to thank the members of the Wireless and Satellite Communications Lab - specifically Hesam Khoshnevis, Mohammad Jabbari Hagh and Farnaz Shayegh - for insightful discussions.

I would like to thank InterDigital Canada Ltée, for funding as well as for valuable feedback on my work. I would also like to acknowledge the financial support of the Fonds Québécois de la Recherche sur la Nature et les Technologies (FQRNT) as well as that of the Electrical Engineering Department of Concordia University.

Last, but certainly not least, I want to thank Vanessa for limitless support and encouragement, through this experience. None of this would have been possible without you Vanessa.

Table of Contents

List of Figures	x
List of Tables	xii
List of Acronyms	xiii
List of Symbols	xiv
CHAPTER 1 Introduction.....	1
1.1 Key Contributions.....	5
1.1.1 Design and Analysis of Variable Time-Fraction Collaborative Communications with no <i>CSIT</i> and perfect <i>CSIR</i>	6
1.1.2 Effect of Imperfect <i>CSIR</i> on Variable Time-Fraction Collaborative Communications	7
1.1.3 Design and Analysis of Variable Time-Fraction Collaborative Communications with Perfect <i>CSIT</i> and <i>CSIR</i>	7
1.1.4 Effect of Imperfect <i>CSIT</i> and <i>CSIR</i> on Variable Time-Fraction Collaborative Communications	8
1.2 Outline of Thesis.....	9
CHAPTER 2 Background and Literature Review	11
2.1 Fading Channel	12
2.1.1 Diversity.....	14
2.1.2 Outage Probability of Direct Transmission Fading Channel.....	14
2.1.3 Probability of Error of Fading Channel	15
2.2 Multiple Antenna Systems.....	16
2.2.1 Performance of Space-Time Codes	17
2.3 Relay Network	17
2.4 Collaborative Communications	18
2.4.1 Two-Phase Collaboration.....	19
2.4.2 Detect-and-Forward	21
2.4.3 Full Diversity Collaboration	22
2.4.3.1 Amplify-and-Forward	22
2.4.3.2 Decode-and-Forward	23
2.4.4 Modifying the Time-Fraction	24
2.4.4.1 Variable Time-Fraction.....	25
2.4.5 Collaborative Coding.....	29

2.4.6 Distributed Space-Time Codes	31
CHAPTER 3 Design and Analysis of Variable Time-Fraction Collaborative Communications	32
3.1 Introduction.....	32
3.2 System Model	34
3.2.1 Code Design.....	36
3.2.1.1 Channel Code Selection.....	38
3.2.1.2 Maximum Likelihood Decoding.....	39
3.2.2 Decoding at the Relay	39
3.2.3 Transmitted SNR	41
3.3 Channel Code Optimization.....	42
3.3.1 Block Codes	46
3.3.2 Convolutional Codes.....	48
3.4 Upper Bound on <i>FER</i>	50
3.4.1 Repetition Encoding.....	51
3.4.2 Using Channel Codes.....	52
3.4.2.1 Modified <i>PEP</i> of Collaborative Modes	53
3.4.2.2 Average <i>FER</i> for Each Collaborative Mode.....	53
3.5 Diversity Advantage	54
3.6 Results.....	56
3.7 Conclusion	64
CHAPTER 4 Effect of Imperfect <i>CSIR</i> on Variable Time-Fraction Collaborative Communications	65
4.1 Introduction.....	65
4.2 System Model	67
4.3 Effect of Imperfect <i>CSIR</i>	67
4.4 <i>PEP</i> with Imperfect <i>CSIR</i>	70
4.4.1 Decoding at the Relay with Imperfect <i>CSIR</i>	70
4.4.2 Decoding at the Destination with Imperfect <i>CSIR</i>	71
4.5 Using Pilot Symbol Assisted Modulation.....	73
4.6 Optimal Number of Pilot Symbols	74
4.7 Results.....	78
4.8 Conclusion	83
CHAPTER 5 Variable Time-Fraction Collaborative Communication with <i>CSIT</i>	84
5.1 Introduction.....	84
5.2 System Model	86

5.3 Outage Probability	88
5.4 Power Allocation Algorithms	88
5.4.1 Basic Power Allocation Algorithm	89
5.4.2 Optimal Power Allocation Algorithm.....	90
5.4.2.1 Diversity Advantage	94
5.4.3 Suboptimal Power Allocation Algorithm	94
5.4.3.1 Diversity Advantage	95
5.5 Results.....	96
5.6 Turbo Coded Collaborative Communications with <i>PAA</i>	103
5.6.1 Results.....	106
5.7 Conclusion	108
CHAPTER 6 Effect of Imperfect <i>CSIT</i> and <i>CSIR</i> on Variable Time-Fraction Collaborative Communication with <i>PAA</i>	110
6.1 Introduction.....	110
6.2 Discussion of Errors.....	111
6.3 Effect of Imperfect <i>CSIT</i>	113
6.3.1 Imperfect <i>CSIT</i> and Perfect <i>CSIR</i>	114
6.3.2 Perfect <i>CSIT</i> and Imperfect <i>CSIR</i>	116
6.3.3 Imperfect <i>CSIT</i> and <i>CSIR</i>	117
6.4 Results.....	118
6.5 Conclusion	124
CHAPTER 7 Conclusion	126
7.1 Future Work	130
7.2. List of Publications	132
References.....	134

List of Figures

Figure 1.1. Collaborative communications model.....	3
Figure 2.1. Network model of collaborative communications.	12
Figure 2.2. Two phases of collaborative communications, a) Exchange phase and b) Collaborative phase.....	20
Figure 2.3. Transmission scenarios, a) Direct transmission, b) Collaboration with source silent in collaborative phase and, c) Collaboration with source transmitting in collaborative phase.....	21
Figure 2.4. Variable time-fraction collaborative communications.	26
Figure 2.5. Outage probability for variable time-fraction collaborative communication with $R = 1/3$	29
Figure 3.1. Three possible modes of collaboration when $B = 3$	37
Figure 3.2. Convolutional encoder for collaborative communications.....	38
Figure 3.3. Two-phase collaborative codes.	43
Figure 3.4. Comparison of upper bound on FER to simulated results for $D_{sr} = 0.3$, $\theta = 0$	57
Figure 3.5. Performance of collaborative communication code with channel codes of varying complexity a) Monte Carlo simulation, b) Upper bound on FER	59
Figure 3.6. $TSNR$ required to achieve $FER=10^{-3}$ for source at origin, and destination at $(1,0)$	60
Figure 3.7. FER performance with source at origin and destination at 1, $\theta = 0$	61
Figure 3.8. Comparison of fixed time-fraction to variable time-fraction for a) Source without feedback, b) Source with simple feedback allowing for constant transmitted power.....	63

Figure 4.1. <i>FER</i> with imperfect <i>CSIR</i> and varying number of pilot symbols for $D_{sr} = 0.3$ and $\theta = 0$	79
Figure 4.2. Required <i>TSNR</i> to achieve $FER=10^{-3}$ with source at origin, destination at 1 and $\theta = 0$	80
Figure 4.3. Gain values for different number of pilot symbols, for all modes when $B = 3$	81
Figure 4.4. Effect of the number of pilot symbols on the required <i>TSNR</i> for different relay locations, $\theta = 0$	82
Figure 5.1. Outage probability of different <i>PAA</i>	97
Figure 5.2. <i>FER</i> for different power allocation algorithms, $D_{sr} = 0.3$ and $\theta = 0$	98
Figure 5.3. The effect of using a variable time-fraction with power allocation algorithms, $D_{sr} = 0.3$ and $\theta = 0$	99
Figure 5.4. Comparison of variable time-fraction to fixed time-fraction for different relay locations, with the source at the origin, destination at 1 and $\theta = 0$, for a) <i>OPAA</i> and b) <i>SPAA</i>	101
Figure 5.5. Comparison of the different <i>PAA</i> algorithms for varying relay locations, with the source at the origin, the destination at 1 and $\theta = 0$	103
Figure 5.6. Block diagram of Turbo coded collaborative communications	104
Figure 5.7. <i>FER</i> performance of Turbo coded variable time-fraction collaborative communications.	107
Figure 5.8. Comparison of Turbo coded collaboration to convolutionally encoded collaboration for different <i>PAA</i> algorithms, and for varying relay locations, with the source at the origin, the destination at 1 and $\theta = 0$	108
Figure 6.1. The effect of imperfect <i>CSIT</i> and perfect <i>CSIR</i> on the performance <i>SPAA</i> , $D_{sr} = 0.3$ and $\theta = 0$	119
Figure 6.2. Effect of the number of pilot symbols on the performance of <i>SPAA</i> with imperfect <i>CSIT</i> and perfect <i>CSIR</i>	120

Figure 6.3. The effect of imperfect *CSIT* and *CSIR* on the performance *SPAA*, $D_{sr} = 0.3$ and $\theta = 0$ 121

Figure 6.4. Effect of the number of pilot symbols on the performance of *SPAA* with imperfect *CSIT* and *CSIR*..... 123

Figure 6.5. Required *TSNR* to achieve $FER=10^{-3}$ for *SPAA* with source at the origin, destination at 1 and $\theta = 0$ 124

List of Tables

Table 3.1. Table of thresholds for each time-fraction at the relay..... 40

Table 3.2. Channel codes for variable time-fraction collaborative communications. 50

Table 4.1. Optimal number of pilot symbols..... 78

List of Acronyms

<i>AF</i>	Amplify-and-Forward
<i>BER</i>	Bit Error Rate
<i>BPAA</i>	Basic Power Allocation Algorithm
<i>CRC</i>	Cyclic Redundancy Check codes
<i>CSIR</i>	Channel State Information at the Receiver
<i>CSIT</i>	Channel State Information at the Transmitter
<i>DF</i>	Decode-and-Forward
<i>FER</i>	Frame Error Rate
<i>MIMO</i>	Multiple-Input Multiple-Output
<i>ML</i>	Maximum Likelihood decoding
<i>OPAA</i>	Optimal Power Allocation Algorithm
<i>pdf</i>	Probability density function
<i>PEP</i>	Pairwise Error Probability
<i>PSAM</i>	Pilot Symbol Assisted Modulation
<i>SNR</i>	Signal-to-Noise Ratio
<i>SPAA</i>	Suboptimal Power Allocation Algorithm
<i>SRDF</i>	Selection Relaying Decode-and-Forward
<i>STC</i>	Space-Time Codes
<i>SVD</i>	Singular Value Decomposition
<i>TSNR</i>	Transmitted Signal-to-Noise Ratio
<i>VTF</i>	Variable Time-Fraction

List of Symbols

$a(d)$	Coefficient of weight enumerating function
$\mathbf{A}(\mathbf{V}, \mathbf{W})$	Square of the codeword difference matrix
B	Number of blocks per frame
$\mathbf{B}(\mathbf{V}, \mathbf{W})$	Codeword difference matrix
C	Codebook
d_i	Hamming distance for i^{th} code segment
d_{\min}	Minimum Hamming distance
D_{ij}	Distance between node i and j
E_s	Symbol energy
$F(Z)$	Weight enumerating function
\mathbf{g}	Convolutional code generator function
G_{ij}	Channel coefficient between node i and j
\hat{G}_{ij}	Estimated channel coefficient between node i and j
H_{ij}	Matrix of fading coefficients between node i and j
k	Number of information symbols
l	Length of each block
L_r	Number of receiving antennas
L_t	Number of transmitting antennas
n	Length of a frame of data
N_o	Complex variance of Additive White Gaussian Noise
m	Memory order of convolutional code
n_p	Number of pilot symbols
n_p^{opt}	Optimal number of pilot symbols
$O(\gamma)$	Order of function
$pdf(G)$	Probability density function of G
$P(d, G)$	Conditional Pairwise Error Probability
$P(d)$	Average Pairwise Error Probability
PG_{ij}	Path gain between node i and j

$P_{out}(\gamma, R)$	Outage Probability
\mathbf{Q}	Covariance matrix of Ξ
R	Data rate
t	Time
\mathbf{V}	Transmitted codeword matrix
\mathbf{W}	Decoded codeword matrix
\mathbf{U}	Unitary matrix used in Singular Value Decomposition
\mathbf{x}_i^j	Transmitted signal from node i during phase j
\mathbf{y}_i^j	Received signal at node i during phase j
\mathbf{z}_i^j	Noise sample at node i during phase j
α	Path loss exponent
γ	Signal-to-Noise Ratio
Δ	Time-fraction
ζ	Power ratio between G and \hat{G}
θ	Angle between the source-destination and source-relay links
λ_{\max}	Maximum eigenvalue
Λ	Matrix of eigenvalues
Ξ	Matrix of estimation error
σ^2	Variance of a random variable
τ	Collaborative threshold
Φ_i^j	Matrix of complex weighting terms for node i during phase j
$\omega(\cdot)$	Modulation mapper

CHAPTER 1

Introduction

With more telecommunications migrating to the wireless domain, efficient wireless transmission methods need to be implemented. Wireless channels differ from wired channels, since they are affected by time-varying multipath fading. The multiplicative effect of fading can lead to severe attenuation of the signal at the destination.

In order to combat fading, wireless communication engineers must increase the diversity of the transmission. Diversity gains are obtained when a message is transmitted through multiple, independent realizations of the channel. Three types of diversity can be achieved in the wireless channel [50, 70]: time diversity, frequency diversity and spatial diversity. In time diversity, the signal is retransmitted at different time intervals in order to be affected by independent realizations of fading. In frequency diversity, the signal is transmitted on several different frequencies, each having independent fading effects. Lastly, spatial diversity can be obtained by transmitting several copies of the signal using multiple transmitting elements at the source. By proper placement of the transmitting

elements, we can ensure that each equivalent sub-channel is affected by independent fading [20, 71]. In all of these methods, the main idea is that we are lessening the likelihood that all transmissions of a signal will be adversely affected by the wireless channel's fading.

Despite the promise that is shown by using multiple transmitting elements to provide spatial diversity, there are some hindrances to full deployment of this technology. Most wireless devices are built for some level of mobility. In the cellular sense, this is obvious, since a mobile handset is designed to function while in motion. However, mobility is also implied in applications such as Wi-Fi; users expect to have terminals (i.e. laptops) that can be easily transported to different locations. Since mobility and transportability impose size restrictions, the requirement for mobility and transportability is an obstacle to having multiple transmitting elements on some wireless equipment. This is especially true when we consider that we must ensure a minimum distance between transmitting elements to provide independent fading elements. Another factor that hinders an increase in the number of transmitting elements is the required power. For example, nodes in a wireless sensor network are constrained by their available power. While using multiple transmitting elements would reduce the necessary transmission power, this can be offset by an increase in complexity of internal circuitry.

As the cost of terminals in wireless networks decrease, their sweeping deployment can be used more advantageously. A new paradigm of wireless communications has been introduced where we allow nearby wireless nodes to collaborate in order to form the equivalent of multiple transmitting elements, in what we call collaborative (or

cooperative) communications [44, 60, 61, 48]. Collaboration provides a method to achieve spatial diversity without requiring multiple antennas at each transmitting node.

A typical collaborative network is given in Fig. 1.1. We have a single-antenna source wishing to transmit data to a destination. A single-antenna relay, idle on the source's channel, is also located in the vicinity. The relay can jointly transmit the source's message, either at different times or simultaneously, with the objective of improving the source's reliability and efficiency. Since the destination uses both the signal from the source and that from the relay when decoding, this is different from multi-hop networking where nodes only process signals coming from a previous node in the route.

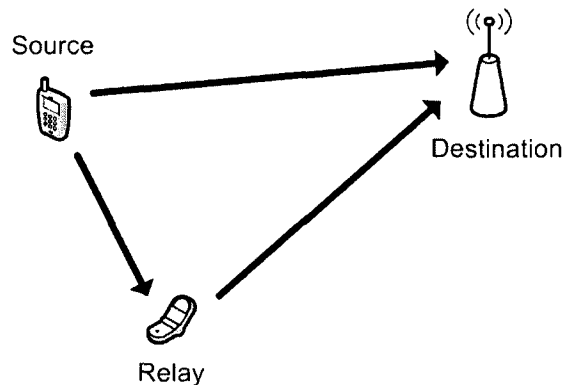


Figure 1.1. Collaborative communications model.

The main advantages of using collaborative communications are:

- Higher spatial diversity: This means that for a specific rate we can decrease the required power. Thus improving the lifespan of wireless nodes.

- Higher bandwidth efficiency: The bandwidth efficiency (measured in b/s/Hz) is increased since for a specific power level, we can increase the modulation and thus the rate of transmission.
- Reduced Interference: Since we can decrease the required transmission power, we can therefore also decrease the interference on other nodes within a wireless network.
- Increased Network Range: By keeping the transmission power and the rate constant, we may increase the distance over which reliable wireless communications can occur.

Because of the reasons enumerated above, collaborative communications is an attractive technology for the future deployment of 4G networks. Fourth generation networks are expected to have seamless connectivity across multiple networks. Collaborative communication can be considered a component of ad hoc networking, where communication need not be point-to-point. As such, using collaboration can be a tool to achieve connectivity between different networks.

Another objective of 4G networks is to achieve high data rates between any two points in the world. Having nearby nodes collaborating with each other significantly increases their useable range. Such a system can ensure connectivity and thus achieve the “anytime, anywhere” credo of 4G networking.

Relaying concepts using some form of collaboration have been proposed to be included in future 4G technologies. Newer releases of the LTE standard (LTE

Advanced) have discussed the use of various concepts for relay nodes. This is also true of future generations of WiMAX such as WiMAX-m.

1.1 Key Contributions

There has been a great amount of work done to provide collaboration in the wireless domain (i.e. [18, 27, 30, 43, 44, 48, 60, 61, 64]). For practical reasons, collaboration in the wireless domain requires a two-phase system. Namely, in the first phase (or exchange phase) the source transmits and the relay listens, while in the second phase (or collaborative phase) the source and relay collaborate to transmit to the destination. The fractional amount of time spent in the first phase is called the time-fraction. Recently it has been shown that using a variable time-fraction can lead to results similar to the genie case of having only a collaborative phase [48]. With that in mind, in this thesis we address the practical implementation as well as the optimization of a collaborative communication protocol using a variable time-fraction. Generally speaking, we provide the design as well as analysis of the performance under different channel state information scenarios: with or without, perfect or imperfect channel state information at the transmitters (*CSIT*) and channel state information at the receivers (*CSIR*).

Following are the key contributions.

1.1.1 Design and Analysis of Variable Time-Fraction Collaborative Communications with no *CSIT* and perfect *CSIR*

First we design a coded collaborative communication protocol which can implement the use of variable time-fractions, when we have perfect *CSIR* and no *CSIT*. We determine a set of available time-fractions from which the relay may select the smallest value which allows it to decode the source's data perfectly. We then provide channel code construction methods such that the relay may collaborate with a specific set of available time-fractions. We discuss the use of *SNR* thresholding values from which the relay decides which time-fraction is most suitable for collaborative communications. We provide the Maximum Likelihood (ML) decoder for variable time-fraction collaborative communication so the destination may use all available information to properly decode the data. Using the codeword difference matrix, as well as the design criteria presented in [70] we provide coding criteria to optimize the performance of collaborative communications with (or without) variable time-fractions. These criteria are applicable to any M-ary communication and to our knowledge this is the first concrete set of design criteria specifically for collaborative communications. We show that for block channel codes using the Alamouti code [2] is optimal. On the other hand, for convolutional codes, our design performs better than space-time coding [70] in the collaborative phase. We then determine the upper bound on the *FER* at the destination. To obtain this upper bound, we develop a new distance metric that is valuable to the study of any layered space-time codes (i.e. when two transmitting elements transmit at the same time). Our upper bound is shown to be very tight when compared to Monte Carlo simulation results. Next, we prove that collaborative communication with variable

time-fraction achieves full spatial diversity. The results show that the performance of collaborative communications using variable time-fraction is better than, or equal to, fixed time-fraction collaboration for any relay location.

1.1.2 Effect of Imperfect *CSIR* on Variable Time-Fraction Collaborative Communications

Second, we study the effect of imperfect *CSIR* in collaborative communications. We study the effect channel estimation error has on the pairwise error probability (*PEP*). We show that the effect is dependent on how many antennas are transmitting at any given moment. Our analysis also shows that imperfect *CSIR* affects the relay's ability to collaborate. This is seen as an increase in the required *SNR* to ensure it can perfectly decode the source's data. We quantify this as an effect on the collaborative thresholds. We then show the effect of imperfect *CSIR* at the destination. It is shown that each phase of communication is affected differently. We provide an analysis of using pilot symbol assisted modulation (*PSAM*) to estimate the channel coefficients. We obtain the optimal number of pilot symbols to minimize the *FER* at the destination. Lastly, we show that the optimal number of pilot symbols is independent of the relay's location.

1.1.3 Design and Analysis of Variable Time-Fraction Collaborative Communications with Perfect *CSIT* and *CSIR*

Third, we study effective methods to use *CSIT* in collaborative communications. We find the outage probability for *CSIT* systems and show that using a power allocation algorithm (*PAA*) is beneficial to the performance of variable time-fraction collaborative

communications. In order to minimize the *PEP*, we provide the design of three *PAA*: basic (*BPAA*), optimal (*OPAA*) and suboptimal (*SPAA*). We show that the *SPAA* can be considered a transmit antenna selection protocol, and that it is much more robust to channel estimation errors than the *OPAA*. The performance of all the *PAAs* is presented. It is shown that for relays located close to the source, the choice of *PAA* is critical. Otherwise, as the relay is moved further from the source towards the destination, all *PAAs* have the same performance, since collaboration becomes less likely. Our results also show that when using *CSIT* variable time-fraction is better than any optimal selection of fixed time-fraction protocols. Next we study the performance of Turbo channel codes in collaboration using *CSIT*. Using [5] we find the weight enumerating function of collaborative Turbo codes with variable time-fraction. Results show that collaborative communications using Turbo coding with simple constituent codes approaches the performance of more complex convolutionally encoded collaborative communications. The negative effects on the collaborative capabilities of the relay are cancelled by the benefits of strong Turbo coding.

1.1.4 Effect of Imperfect *CSIT* and *CSIR* on Variable Time-Fraction Collaborative Communications

Lastly, we study the effect of imperfect *CSIT/CSIR* when using the *SPAA*. We discuss the possible sources of error when channel coefficients need to be estimated. We study the hypothetical case of imperfect *CSIT* and perfect *CSIR*. We show that the effect of imperfect *CSIT* is manifested as potentially selecting the wrong node from which to transmit from in the collaborative phase. We quantify the effect as a probability of

antenna selection that is less likely to be erroneous as the number of pilot symbols or the SNR increase. We also show the realistic effect of having both imperfect $CSIT$ and $CSIR$. It is shown that when using an $SPAA$ it is conceivable that the error at the transmitters and that at the receivers will be the same. Therefore, our results show that the effect of imperfect $CSIT$ and $CSIR$ for $SPAA$ is similar to only imperfect $CSIR$ in systems without the use of $CSIT$. We show the effect of relay location for the system with imperfect $CSIT$ and perfect $CSIR$. On the other hand, our results show that for a system with imperfect $CSIR$ and $CSIT$, the optimal number of pilot symbols is independent of the relay's location. We analytically obtain the optimal number of pilot symbols to minimize the FER of the over-all transmission.

1.2 Outline of Thesis

In Chapter 2 we present a literature review of topics related to the development of collaborative communications. We also present some background information useful for the study of variable time-fraction collaborative communications. Chapter 3 presents the development of variable time-fraction collaborative communications. We provide the design as well as the analysis of the performance of variable time-fraction collaborative communications. The study of the effect of imperfect $CSIR$ is presented in Chapter 4. Here the effect on the FER performance is examined and the use of $PSAM$ is analyzed. In Chapter 5 we discuss the use of $CSIT$. We provide an analysis of different $PAAs$ to optimize the performance when using $CSIT$. Next, Chapter 6 provides results on the

effect of imperfect *CSIT* and *CSIR* when using the *SPAA*. Lastly, in Chapter 7 we provide some concluding remarks as well as a discussion of possible future work.

CHAPTER 2

Background and Literature Review

The wireless network under study in this thesis is the three-terminal network with one source, one relay and one destination, given by Fig. 2.1. The values of D_{ij} , \mathbf{H}_{ij} and PG_{ij} denote the distance, matrix of fading coefficients and path gain, respectively, between nodes i and j . We assume the source wishes to transmit data to the destination and that the relaying node is otherwise idle on the specific wireless channel, and may be used to improve the performance of the source-destination link.

The following notation is used throughout this thesis: italic letters (x) represents scalar quantities, bold lowercase letters (\mathbf{x}) represent vectors, bold uppercase letters (\mathbf{X}) represent matrices, $(\cdot)^T$ denotes transpose, $(\cdot)^\dagger$ denotes conjugate transpose, $\|\cdot\|^2$ denotes the Frobenius norm of a matrix, $tr(\cdot)$ denotes the trace of a matrix, $E_x[\cdot]$ denotes the expectation operator with respect to random variable x , $\mathcal{N}(\mu, \sigma^2)$ represents the

Gaussian distribution with mean μ and variance σ^2 and $\mathcal{C}(\mu, \sigma^2)$ represents the circularly symmetric complex Gaussian distribution with variance $\sigma^2 / 2$ per dimension.

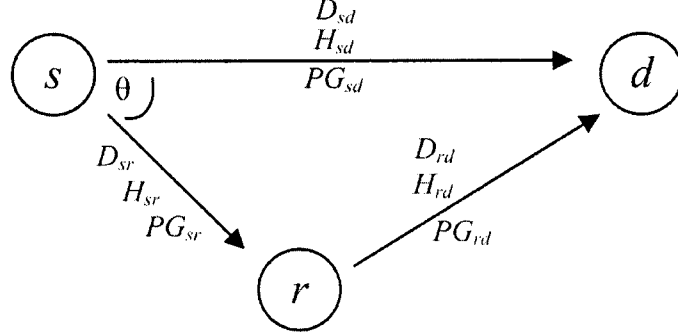


Figure 2.1. Network model of collaborative communications.

2.1 Fading Channel

The wireless channel is impaired by both Additive White Gaussian Noise (AWGN) and, more importantly, fading. The fading is represented as a multiplicative gain on the transmitted signal. In this thesis we use the multipath fading model with the assumption we have a large number of scatterers. In such a case, we can invoke the central limit theorem and we have a Gaussian process model for the channel impulse response [56]. We can therefore write the fading terms between nodes i and j , as $h_{ij} \sim \mathcal{C}(0, \sigma_{ij}^2)$, where we select the complex variance of the fading terms, $\sigma_{ij}^2 = 1$. The probability distribution function of the envelope of the fading terms, given by $pdf(|h_{ij}|)$ is,

$$pdf(|h_{ij}|) = \frac{2|h_{ij}|}{\sigma_{ij}^2} e^{-\frac{|h_{ij}|^2}{\sigma_{ij}^2}}, \quad |h_{ij}| \geq 0 \quad (2.1)$$

and the phase is uniformly distributed in the interval $(0, 2\pi)$.

In this thesis, we assume the fading terms to be constant over an entire frame of data, referred to as block fading. The length of time over which the channel is assumed constant is referred to as the coherence time. Therefore in our model we assume the coherence time to be greater than the frame length n .

To consider the effect of node positioning, we use the concept of large scale fading by introducing the path gains, PG_{ij} . Like the fading coefficients, the path gain is a multiplicative gain on the transmitted signal. To determine the actual value of the path gains, we require intimate knowledge of the environment where the network would be deployed. However, we obtain results that can be scaled to the proper implementation levels by using the idea of a normalized unit of distance. We set the distance between the source and destination to be equivalent to one unit ($D_{sd} = 1$) and to have $PG_{sd} = 1$. From this we may determine other path gains by using a path loss exponent α . All path gains are obtained from,

$$PG_{ij} = \left(\frac{D_{sd}}{D_{ij}} \right)^\alpha PG_{sd}. \quad (2.2)$$

We can now define the channel coefficients as being the multiplicative gain which combines both the effect of fading coefficients and path gain. Namely, we have as channel coefficient, $G_{ij} = \sqrt{PG_{ij}} h_{ij}$.

In a fading wireless channel, the received signal at node j from node i is given by

$$y = \sqrt{E_s} G_{ij} x + z, \quad (2.3)$$

where x represents the transmitted symbol of unit energy and z represents the AWGN term with $z \sim \mathcal{C}(0, N_0/2)$. Much of the advancements in our understanding of the fading channel have been summarized in [9].

2.1.1 Diversity

In order to improve the performance of the fading channel, we wish to use methods to increase diversity. Diversity means receiving the data through independently faded channels such that the probability of only receiving corrupted signals is decreased. There are many methods which may be used to achieve diversity [56,57], such as transmitting the same signal at different times, using different frequencies or through different spatial channels, all of which should have independent fading coefficients.

We quantify diversity by saying a scheme achieves diversity i , if the following holds [12],

$$\lim_{\gamma \rightarrow \infty} \frac{\log P_e(\gamma)}{\log \gamma} = -i, \quad (2.4)$$

where $\gamma = \frac{E_s}{N_0}$ and $P_e(\gamma)$ is the probability of error.

2.1.2 Outage Probability of Direct Transmission Fading Channel

For comparative purposes, in this section we provide results pertaining to direct transmission of data from the source to the destination.

An outage event is defined as a channel realization where a specific rate of transmission cannot be supported by the wireless link. For Rayleigh fading, at high

signal-to-noise ratio (SNR), the outage probability of the (s, d) link is approximated by [44],

$$P_{out}^{direct}(\gamma, R) \approx \frac{1}{PG_{sd}} \frac{2^R - 1}{\gamma}, \quad (2.5)$$

where R is the desired rate of transmission. Since the outage probability is proportional to γ^{-1} , we see that direct transmission has unit diversity.

2.1.3 Probability of Error of Fading Channel

We may wish to obtain the probability of error when transmitting through a fading channel. When using channel coding, we may use the pairwise error probability (PEP) conditioned on the Hamming distance between two codewords, d , and the fading coefficient, G_{ij} , given by

$$P(d, G_{ij}) = Q\left(\sqrt{\frac{2E_s d |G_{ij}|^2}{N_o}}\right), \quad (2.6)$$

where we have used the Q-function, which is the tail probability of the normalized Gaussian distribution, and we have assumed antipodal signaling.

We can obtain the average PEP , by averaging over all fading coefficients,

$$P(d) = \int_{G_{ij}} P(d, G_{ij}) pdf(G_{ij}) dG_{ij}, \quad (2.7)$$

where we can find $pdf(G_{ij})$ from the definition of G_{ij} , which is a complex Gaussian,

$$pdf(G_{ij}) = pdf(\theta_{G_{ij}}) pdf(|G_{ij}|) = \frac{1}{2\pi} \frac{2|G_{ij}|}{PG_{ij}} e^{-\frac{|G_{ij}|^2}{PG_{ij}}}, \quad |G_{ij}| \geq 0, \quad 0 \leq \theta_{G_{ij}} < 2\pi. \quad (2.8)$$

2.2 Multiple Antenna Systems

We can obtain spatial diversity by using physical antenna arrays at either the transmitters or receivers. Such a scenario is named multiple-input multiple-output (MIMO) communication. The advantage of using MIMO is a well studied problem [2, 20, 51, 68, 70, 71]. In such cases, instead of trying to mitigate the inherent fading associated with the wireless channel, wireless network designers use it to their advantage. There has been much work on determining the performance limits of MIMO channels [8, 20, 51, 71, 82, 88], which show that significant capacity improvements can be achieved.

To exploit the increase in capacity, we use the redundancy introduced by additional antennas. Two goals are targeted, multiplexing gain and diversity gain. On the one hand we may use a multiplexing method such as BLAST [19, 83], which in essence uses the MIMO channel as a combination of several SIMO (single-input multiple-output) channels, each responsible for an independent data stream. At the other end of the spectrum lie methods [2, 70] such as Space-Time Codes (STC) which ensure the maximum available spatial diversity is achieved. It is shown in [23, 70] that the maximum spatial diversity achievable is given by the product of the number of transmitting antennas with the number of receiving antennas.

The trade-off between both goals is shown in [88]. Specifically it is shown that when each additional antenna is introduced in a MIMO system, it can be used either to increase the diversity gain or the multiplexing gain, but not both at the same time.

2.2.1 Performance of Space-Time Codes

Space-time codes have been developed to provide methods to ensure full spatial diversity can be achieved [23, 68, 70]. The received signal at node j from node i is given by,

$$\mathbf{y}_j = \sqrt{E_s} \mathbf{G}_{ij} \mathbf{x}_i + \mathbf{z}_j \quad (2.9)$$

where \mathbf{y}_j is a $L_r \times 1$ vector, \mathbf{x}_i is a $L_t \times 1$ vector, \mathbf{z}_j is a $L_r \times 1$ vector of noise elements, L_t and L_r represents the number of transmitting and receiving elements, respectively.

We provide the *PEP* when codeword matrix \mathbf{V} is transmitted and codeword matrix \mathbf{W} is decoded,

$$P(\mathbf{V}, \mathbf{W}, \mathbf{G}_{ij}) = Q \left(\sqrt{\frac{E_s \|\mathbf{G}_{ij} (\mathbf{V} - \mathbf{W})\|^2}{2N_o}} \right), \quad (2.10)$$

where $P(\mathbf{V}, \mathbf{W}, \mathbf{G}_{ij})$ represents the *PEP* between codewords \mathbf{V} and \mathbf{W} for a MIMO channel between nodes i and j with channel matrix \mathbf{G}_{ij} .

2.3 Relay Network

The problem of collaboration has its roots in the study of the classical relay channel [15, 78, 79]. Relay channels have the traditional source and destination, as well as an extra terminal named the relay. These relay nodes receive, process and retransmit the source's data so as to improve the capacity provided by simple source-destination networks. The relay's transmitted signal can be any arbitrary function of its past received signals. Most

of the initial work done on the relay channel deals with AWGN channels and provides capacity calculations [16].

Three terminal communication channels were introduced in [78, 79]. This work was further expanded on by Cover and El Gamal [15] who developed lower and upper bounds on the channel capacity using information theoretic concepts.

The study of relay networks further progressed to include situations where the channels are wireless [86]. In this case, factors such as distance of nodes as well as interference play a factor. Wireless relaying is also studied in [25] where the half duplex constraint is used. Namely, nodes can't receive and transmit on the same wireless channel. The reduction in capacity from using the half duplex constraint is found to be minimal. Other prominent works on relaying and coding over the relay channel include [1, 6, 14, 41, 42, 80].

2.4 Collaborative Communications

Around the turn of this century, researchers realized that relaying can be used to mimic multiple antenna systems even when the wireless nodes are incapable of having multiple antennas. This led to the development of collaborative (or cooperative) communications. In this new paradigm, sources help each other by forming virtual antenna arrays to the destination. Much work has been put into this new model of wireless communications, including capacity results [26, 27, 42] and the development of protocols to achieve this capacity e.g. [18, 22, 30, 32, 43, 44, 48, 60, 61, 66].

In this section we present an overview of the main results on collaborative communications that apply to the work given in this thesis.

2.4.1 Two-Phase Collaboration

Due to causality, the relay in collaborative communication is unaware of the source's data at the beginning of each frame. Therefore, the relay has two operations to perform: it must listen to the signal from the source and then it must transmit another signal to the destination. If we consider the nodes to be "cheap" [39], then transmission and reception in the same frequency band is not possible, due to limitations in radio implementation. Severe attenuation over the wireless channels, along with insufficient electrical isolation between the receiver and transmitter circuitry in the relay mean that any signal transmitted from a node will overwhelm any received signal. To deal with this, the so-called half-duplex constraint is assumed. Due to this constraint, two-phase protocols are proposed for collaboration.

In a two-phase protocol, the relay spends the first phase (also referred to as the exchange phase) receiving the data from the source. In the second phase (also known as the collaborative phase), the relay transmits its own signal to the destination, see Fig. 2.2. In the second phase, the source may or may not continue transmitting a signal. Depending on the protocol under study, the destination may listen only to the collaborative phase or both phases to perform decoding. Two-phase protocols eliminate the need for the relay to collaborate through a different wireless channel. However, there is still an increase in the bandwidth requirement. It is evident that any signal sent by the

source will require twice the bandwidth (twice the time) for the relay to be able to collaborate.

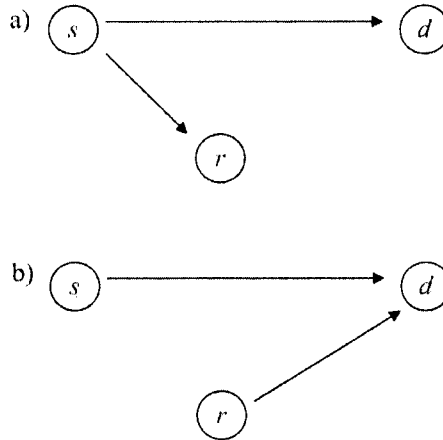


Figure 2.2. Two phases of collaborative communications, a) Exchange phase and b) Collaborative phase.

When we compare collaboration to traditional direct transmission, as in Fig. 2.3, we see that for collaboration, the entire data transmitted from the source must be contained in a fraction of the channel allocation used in direct transmission. Note that this collaborative fraction (referred to as time-fraction), n/n , need not be $1/2$. We also see that in the collaborative phase, the source may or may not continue transmitting its signal (in the form of parity or repetition).

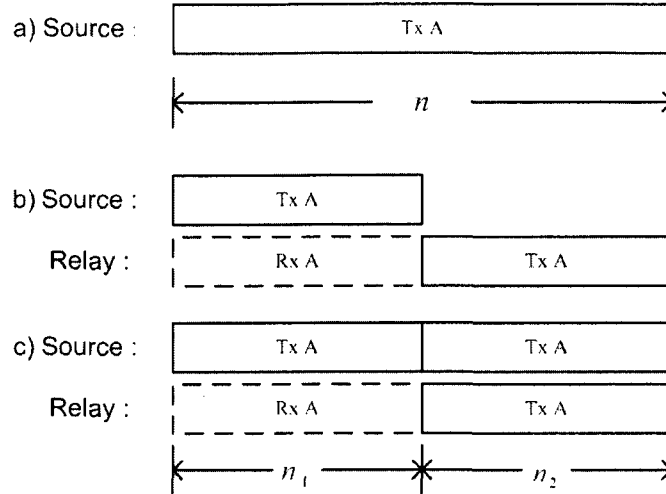


Figure 2.3. Transmission scenarios, a) Direct transmission, b) Collaboration with source silent in collaborative phase and, c) Collaboration with source transmitting in collaborative phase.

Several collaborative communication protocols have been proposed within the framework of two-phase communication.

2.4.2 Detect-and-Forward

The idea behind two-phase communication to achieve collaboration was first proposed in [60, 61]. The method proposed has the relay attempt to detect the transmitted symbols from the source and then retransmit the detected symbols in the collaborative phase. In [60, 61], there is a trade-off between the amount of symbols that are transmitted with collaboration and those transmitted without, in order to diminish the loss in throughput brought about by collaboration. As a simple example, in the first and second channel uses, the source transmits two symbols, while in the third channel use, the source and relay retransmit the second symbol.

This method provides a simple way to achieve collaboration in the wireless channel. However, it has some drawbacks. Firstly, if detection at the relay is incorrect, collaboration can be detrimental to the eventual detection at the destination. In addition, to achieve optimal decoding, the destination needs to be aware of the inter-user channel characteristics. More important, however, is the predicament caused by the trade-off to increase throughput. The error rate performance of a system is dominated by the worst case scenario. In this case, the symbols that are transmitted with collaboration can achieve full diversity, whereas those transmitted without collaboration can only ever achieve unit diversity. Therefore, the over-all performance of this method does not maximize diversity, and hence cannot be assumed to maximize throughput.

2.4.3 Full Diversity Collaboration

To ensure full diversity when using collaborative communications, several collaborative communication protocols, named cooperative diversity protocols, are proposed in [44]. In [44], collaborative protocols require that only the relay transmits in the collaborative phase, while the source remains silent.

2.4.3.1 Amplify-and-Forward

The simplest method to achieve collaboration in the wireless channel is for the relay to listen to the source's signal, then simply amplify the signal and transmit it to the destination. This method is named Amplify-and-Forward (AF). AF is basically a version of repetition encoding, where the source and relay transmit the same thing; except that here the relay's signal is corrupted by its own noise.

To ensure power constraints are met, the relay scales the signal it receives from the source accordingly. This is achieved assuming the relay can estimate G_{sr} with high accuracy.

For Rayleigh fading, the outage probability of AF is approximated at high SNR to be [44],

$$P_{out}^{AF}(\gamma, R) \approx \left(\frac{1}{2PG_{sd}} \frac{PG_{sr} + PG_{rd}}{PG_{sr}PG_{rd}} \right) \left(\frac{2^{2R} - 1}{\gamma} \right)^2, \quad (2.11)$$

which shows full spatial diversity of order 2 is obtained since the outage probability is proportional to γ^{-2} . Even though noise is amplified at the relay, the destination receives two copies of the signal through two independently faded channels, which maximizes the spatial diversity. Further results on the performance of the AF method for collaboration have been presented in [3, 49, 84].

2.4.3.2 Decode-and-Forward

As is implied in the name of Decode-and-Forward (DF), this method requires the relay to decode the data transmitted by the source, re-encode it and transmit it to the destination in the collaborative phase. This extra step removes the effect of transmission errors in the source-relay channel. However, this improvement comes with more complexity at the relay.

In the derivation of the outage probability, a condition is placed on the relay [44]. It is required that the relay be able to fully decode the source's data without error in order to have a successful transmission. For Rayleigh fading, the outage probability of DF is approximated at high SNR by,

$$P_{out}^{DF}(\gamma, R) \approx \frac{1}{PG_{sr}} \left(\frac{2^{2R} - 1}{\gamma} \right). \quad (2.12)$$

Since the performance of DF is limited by the performance of the (s, r) channel, (2.12) shows that in this strict sense, DF does not achieve full diversity.

In order to overcome the shortcomings of DF, selection relaying decode-and-forward (SRDF) is proposed in [44]. In this case, when the relay is unable to decode the source's signal, the source falls back to direct transmission for the remainder of the frame, while the relay remains silent. For the case of repetition coding in the collaborative phase, the outage probability for SRDF in a Rayleigh faded environment is approximated at high SNR by [44],

$$P_{out}^{SRDF}(\gamma, R) \approx \left(\frac{1}{2PG_{sd}} \frac{PG_{sr} + PG_{rd}}{PG_{sr}PG_{rd}} \right) \left(\frac{2^{2R} - 1}{\gamma} \right)^2. \quad (2.13)$$

Therefore, the outage probability of SRDF is identical to that for AF at high SNR . This means that SRDF achieves full spatial diversity, since it is not limited by the performance of the (s, r) channel. Further results studying the effect of using the DF method are presented in [32, 33, 66].

2.4.4 Modifying the Time-Fraction

The fraction of time that a two-phase protocol resides in the exchange phase need not be half of the total time. Suppose we wish to transmit data at a rate R bits per second in n channel uses. We may split the number of channel uses unevenly for each phase, such that $n = n_1 + n_2$. The time-fraction is defined as the ratio of the time spent in the exchange phase versus the over-all time. We have as time-fraction,

$$\Delta = \frac{n_1}{n}. \quad (2.14)$$

To maintain a constant over-all rate R , each phase is operated with rates R_1 and R_2 .

In the simplest example, no channel coding is done in either phase. Therefore, each phase must contain the same information (possibly with different coding rates) in order to ensure all data achieves full spatial diversity. We therefore select,

$$R_1 n_1 = R_2 n_2. \quad (2.15)$$

In [52], it is shown that several different collaborative protocols using SRDF can achieve full spatial diversity at high SNR , regardless of the time-fraction selected.

2.4.4.1 Variable Time-Fraction

The ability to modify the time-fraction means that we may be inclined to spend less time in the exchange phase and have both the source and relay transmit in the collaborative phase. The performance at the destination can therefore be improved due to the increase in collaboration. However, there is a cost associated with decreasing the time-fraction. Either we need to increase the energy from the source to ensure that a higher rate (s, r) link can still be of high enough quality to allow for collaboration, thus increasing the over-all power requirements. Otherwise we suffer from a lack of collaboration from the relay, thus minimizing the potential gain promised by collaborative diversity.

In [47, 48], a bandwidth-efficient protocol without pre-determined fixed time-fractions is presented. Through an information theoretic approach, it is shown that allowing the relay to determine its own time-fraction, based on the (s, r) channel coefficients, we can ensure the collaboration time is maximized. This is shown to

improve the Bit Error Rate (*BER*) performance to within a few dBs of the “genie” case; a case where the relay is allowed to collaborate from the beginning of each frame.

In this method, the source transmits a signal for the duration of the frame length. On the other hand, the relay listens until it can successfully decode the signal and then begins transmitting its own signal to the destination, as in Fig. 2.4. The signals received during both phases and from both source and relay, are used at the destination for decoding.

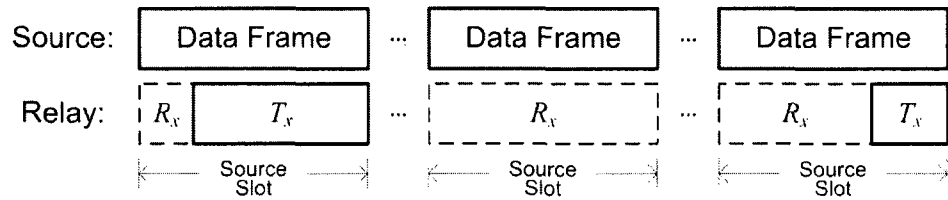


Figure 2.4. Variable time-fraction collaborative communications.

A MIMO system with Gaussian codebook and rate R can reliably communicate over a channel with channel gain matrix \mathbf{G} as long as,

$$R < \log_2 \det(I + \gamma \mathbf{G} \mathbf{G}^\dagger) \triangleq C(\mathbf{G}), \quad (2.16)$$

where I denotes the identity matrix.

The relay must be able to decode the entire transmitted codeword during the first phase of communication. This means the relay must decode nR bits in n_1 channel uses. Since the relay is aware of its received channel, it can select the time-fraction Δ such that $nR < n_1 C(\mathbf{G}_{sr})$. At the destination, the data is received at a rate of $C(\mathbf{G}_{sd})$ bits per channel use in the exchange phase and $C(\mathbf{G})$ bits per channel use in the collaborative

phase; where we have used $\mathbf{G} = [\mathbf{G}_{sd} : \mathbf{G}_{rd}]$. Since the destination uses the signals received in both phases to decode, it may reliably decode the data if $nR < n_1 C(\mathbf{G}_{sd}) + (n - n_1) C(\mathbf{G})$.

Using the discussion in the previous paragraph, we provide the achievable rate, modified from [48] to include the specific effect of node locations,

$$R \leq \Delta C(\mathbf{G}_{sr}) \text{ and } R \leq \Delta C(\mathbf{G}_{sd}) + (1 - \Delta) C(\mathbf{G}), \quad (2.17)$$

where $0 < \Delta < 1$, or

$$R \leq \Delta C(\mathbf{G}_{sd}). \quad (2.18)$$

To determine the outage probability of the variable time-fraction protocol, we define an outage event as

$$E_o = [R > \Delta C(\mathbf{G}_{sd}) + (1 - \Delta) C(\mathbf{G})]. \quad (2.19)$$

Therefore, the outage probability, defined as the probability over all channel realizations, to experience an outage event, is given by [48],

$$P_{out}^{VTF} = \Pr [R > \Delta C(\mathbf{G}_{sd}) + (1 - \Delta) C(\mathbf{G})], \quad (2.20)$$

where VTF stands for variable time-fraction.

The *SNR* at the destination is dependent on the relative location of the source and relay. As the relay moves, the same transmitted energy will not lead to the same received signal energy. Therefore, *SNR* does not provide a fair comparative metric. We wish to have a metric that will properly equate the energy used by two different transmission strategies so that they can be compared. In order to do this we introduce the concept of transmitted *SNR*, or *TSNR*, defined as the ratio between the total transmitted signal power to the noise power at the receiver. The transmitted energy per symbol for each channel

realization is expressed as $(2 - \Delta)E_s$, hence the averaged $TSNR$ of the over-all network is given by

$$TSNR = \frac{(2 - E[\Delta])E_s}{N_o}, \quad (2.21)$$

where $E[\Delta]$ is the average time-fraction over all channel realizations.

Figure 2.5 shows the outage probability of a $R=1/3$ collaborative communication system with $D_{sr} = 0.3$, $\theta = 0$ or $D_{sr} = 0.7$, $\theta = 0$, where θ is the angle between the (s, d) and (s, r) links as defined in Fig. 2.1. For comparison, we provide the outage probability of direct transmission. It is evident from the steeper outage probability slope that collaboration provides greater diversity than direct transmission. We also provide “genie” results where we assume the relay is able to collaborate at the beginning of each frame since it is given the transmission data beforehand. The loss between the genie case and the realistic case is not very big when the relay is near the source ($D_{sr} = 0.3$). On the other hand, when the relay is close to the destination, we see the loss – due to the relay being required to listen in the first phase – is much more evident. With a relay located close to the destination, if it were able to collaborate at the beginning of each frame, the system would require 5 dB less $TSNR$ to achieve the same outage. As expected, the genie case for a relay close to the destination is much greater than that for a relay near the source. That is because a relay with the same collaborative capabilities will provide more gain as it approaches the destination.

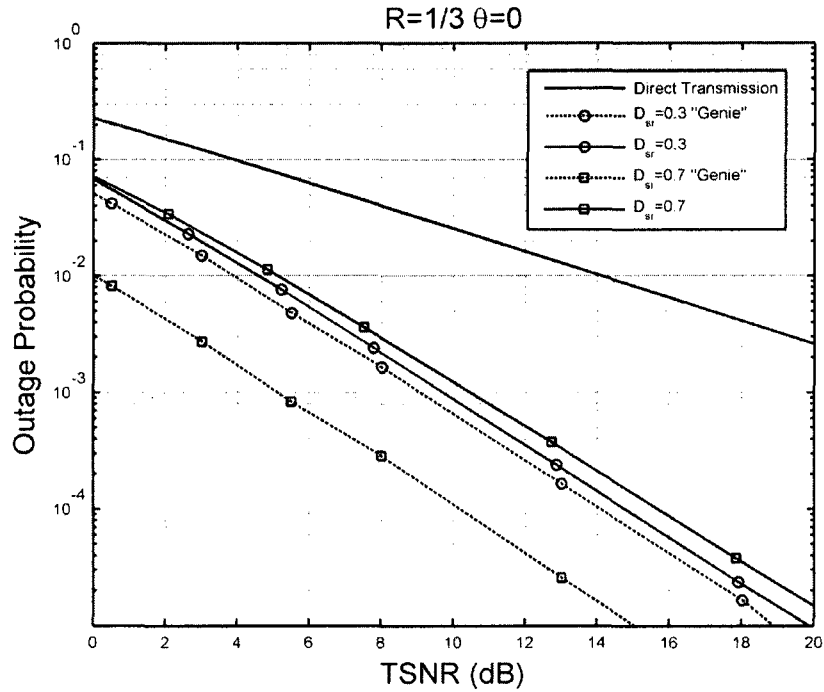


Figure 2.5. Outage probability for variable time-fraction collaborative communication with $R = 1/3$.

2.4.5 Collaborative Coding

The promise of spatial diversity gains from collaborative communications led to the development of practically achievable collaborative communication protocols. Collaborative (or cooperative) coding [30, 31, 34, 64] was developed by incorporating channel coding together with collaboration. In coded collaboration, different portions of the codeword to be transmitted are sent via the source and relay's independently faded wireless channels.

At its simplest, the source encodes its data with a high rate channel code. The relay receives the codeword and decodes the information bits. Either by the use of cyclic redundancy check (CRC) codes or by thresholds on its received SNR , the relay decides if

decoding the codeword will provide a reliable determination of the information bits. If so, the relay re-encodes the information bits, obtaining a new set of parity bits to be transmitted to the destination. At the destination, the combination of parity bits obtained in the first phase from the source, as well as parity bits obtained in the second phase from the source and/or relay, is used to obtain optimal decoding.

Different coding strategies may be used within this collaborative framework. Block and/or convolutional coding may be used at both the source and relay. In order to separate the codewords into two phases, puncturing, product codes or other forms of concatenation may be used.

In [30], the *PEP*, averaged over all channel coefficients using the method of [63] is upper-bounded by

$$P(d_1, d_2) \leq \frac{1}{2} \left(\frac{1}{1 + d_1 \gamma P G_{sd}} \right) \left(\frac{1}{1 + d_2 \gamma P G_{rd}} \right), \quad (2.22)$$

where d_1 and d_2 are the Hamming distances between two codewords in the exchange and collaborative phases respectively. At high *SNR*, the *PEP* is proportional to γ^{-2} , given that neither d_1 nor d_2 are zero. Therefore, coded collaboration achieves full spatial diversity under specific coding criterion, given that the relay is able to collaborate.

Using the recent advances in technology, the promise of relaying as a form of collaboration is very real. A large amount of work has been carried out to develop practical collaboration schemes to achieve the gains promised by information theory. Some of these results are found in [10, 11, 30, 31, 38, 72, 73, 74, 87].

2.4.6 Distributed Space-Time Codes

In order to further improve the performance of collaboration, the use of multiple relays was introduced in [43]. In so-called distributed space-time codes, the source transmits its message in the exchange phase, while the available relays listen. In the collaborative phase, the relays who can reliably decode the message without error, re-encode the data using a space-time code. In such a case, the maximum spatial diversity, given by the total number of relays plus one (for the source), can be achieved without a further increase in bandwidth requirements. Recent results on distributed space-time coded protocols can be found in [4, 35, 36, 58, 59, 76].

CHAPTER 3

Design and Analysis of Variable Time-Fraction Collaborative Communications

3.1 Introduction

In this chapter, we present a collaboration strategy, using channel coding to achieve variable time-fractions depending on the instantaneous channel characteristics. This work can be considered a general solution to the two-phase collaboration problem using the selection relaying decode-and-forward (SRDF) strategy. Works such as [30, 64, 66], can be considered specific implementations of the solution provided in this chapter. Unlike previous use of channel coding in collaborative schemes [30], the strategy developed here makes better use of the instantaneous channel resources at any given time and is shown to be more robust to different relay locations.

The time-fraction of a collaborative protocol is defined as the percentage of time spent in the exchange phase. To enable the use of variable time-fractions, dependent on

the channel realizations, the relay listens until it has achieved a specified decoding criterion, then re-encodes and transmits new parity symbols. Each possible time-fraction is known as a mode of collaboration.

After presenting the proposed variable time-fraction collaborative communications protocol, we discuss code design methods. It is from the proper design of the code that we can have variable time-fractions at the relay. We show how both the relay and destination can each decode the data, depending on the time-fraction. Next we discuss code optimization. In this chapter we assume full *CSIR* and no *CSIT*. From this assumption we develop criteria to optimize the channel code used in collaborative communications.

In order to better study the performance of variable time-fraction collaborative communication, we provide an analysis to determine the Frame Error Rate (*FER*). To obtain the *FER* we develop new strategies to study the performance of any layered space-time code.

Our results show that even though the relay cannot collaborate all the time, we can achieve full diversity at high signal-to-noise ratio. We further prove this analytically by studying the obtained upper bound on *FER*.

To further validate the use of a variable time-fraction, we compare the proposed protocol to ones with fixed time-fraction. Our results show that variable time-fraction collaboration outperforms fixed time-fraction collaboration for all relay locations, and is thus deemed more robust.

The rest of the chapter is organized as follows; Section 3.2 provides the system model. Section 3.3 discusses methods to optimize the channel code used in collaboration.

Section 3.4 provides the analysis to obtain an upper bound on the *FER*. In Section 3.5, we prove that collaborative communications with variable time-fraction achieves full spatial diversity. Section 3.6 gives some results on the performance of collaborative communications with variable time-fraction. Finally Section 3.7 gives some concluding remarks.

3.2 System Model

The purpose of collaborative communication is to enable single antenna terminals to achieve higher diversity. Therefore, each node in Fig. 2.1 is equipped with one antenna, and we can write the fading coefficient as h_{ij} . To determine the path gains, we assume the distance between s and d is normalized ($D_{sd} = 1$) and its path gain is set to 0 dB. The relay can be located anywhere in the two-dimensional plane. Therefore all other path gains are calculated using their relative distances and a path loss exponent of 2 [57].

In this chapter, the transmitting ends of all the nodes do not have access to *CSIT*. Due to this criterion, the source is considered blind – meaning it is unaware of when the relay is helping it. The source’s blindness means that it transmits a signal for the entire frame of communication (during both phases). On the other hand, all receiving ends of the nodes have knowledge of *CSIR*. This means the destination is not only aware of the fading coefficients and path gains of its received channels, but is also aware of the collaborating status of the relay. Access to *CSIR* at the relay is used to determine the time-fraction for each channel realization.

The entire frame of communication is assumed to be of length n , and the time-fraction is denoted by Δ , where $0 < \Delta \leq 1$. During the exchange phase, both the relay and destination receive signals,

$$\mathbf{y}_r^e = \sqrt{E_s} G_{sr} \mathbf{x}_s^e + \mathbf{z}_r^e, \quad (3.1)$$

$$\mathbf{y}_d^e = \sqrt{E_s} G_{sd} \mathbf{x}_s^e + \mathbf{z}_d^e, \quad (3.2)$$

where \mathbf{y}_i^e denotes the $1 \times n\Delta$ vector of received signals at node i , \mathbf{x}_s^e denotes the $1 \times n\Delta$ vector of transmitted unit-energy symbols from the source, \mathbf{z}_i^e denotes the $1 \times n\Delta$ noise vector at node i with $z_i^e \sim \mathcal{C}(0, N_o)$, E_s is the energy of the transmitted symbols, and $G_{ij} = \sqrt{PG_{ij}} h_{ij}$ denotes the channel coefficients for link (i, j) , where the quasi-static fading coefficients h_{ij} are constant during a frame with $\mathcal{C}(0, 1)$. In the collaborative phase, the source and relay collaborate to transmit to the destination,

$$\mathbf{y}_d^c = \sqrt{E_s} \mathbf{G} \mathbf{X}^c + \mathbf{z}_d^c, \quad (3.3)$$

where \mathbf{y}_d^c and \mathbf{z}_d^c are $1 \times n(1-\Delta)$, $\mathbf{G} = \left(\sqrt{PG_{sd}} h_{sd}, \sqrt{PG_{rd}} h_{rd} \right)$ is a vector of channel coefficients, and the $2 \times n(1-\Delta)$ matrix $\mathbf{X}^c = \left[\mathbf{x}_s^c, \mathbf{x}_r^c \right]^T$. Throughout this work we use superscript “ e ” to denote the exchange phase and “ c ” to denote the collaborative phase.

At the destination, the data received during both phases is used to decode the transmitted data. It is shown in Section 3.3 that this allows for a wider variety of coding options in the collaborative phase.

3.2.1 Code Design

The source's blindness imposes specific code design criterion on the encoding process. The source is unaware of the relay's collaboration status, therefore it cannot encode according to each collaborative mode. Instead it encodes the data using a channel code under the assumption that the destination only receives a signal from the source. As such it uses coding strategies available to any traditional point-to-point wireless transmission.

At the relay, the code design depends on the set of available time-fractions. In [48], the set of time-fractions is given by the set of real numbers such that $0 < \Delta \leq 1$. This leads to solving for the optimal time-fraction. That is not feasible in practice since it would require infinite n to allow for real-valued time-fractions. Instead, we use a finite set of quantized time-fractions, $\Delta \in \{\Delta_1, \Delta_2, \dots, 1\}$, where we assume the set is ordered such that $\Delta_i < \Delta_j$ if $i < j$, and $\Delta = 1$ means that the relay is unable to collaborate for this specific channel realization.

The set of time-fractions is further constrained to ensure that there is no bandwidth expansion. We wish to transmit k information bits in n time periods. We require that the relay be able to fully decode the information during the exchange phase. Therefore to ensure the lowest time-fraction is valid, the k information bits must be represented in the first $n\Delta_1$ symbols. To ensure there is no bandwidth expansion, we require a modulation with at least $2^{\frac{k}{n\Delta_1}}$ constellation points. Also, the difference between two time-fractions should be large enough to make certain that the larger time-fraction allows at least one more symbol to be transmitted during the exchange phase when compared to the smaller one. We say $\Delta_j - \Delta_i \geq \frac{1}{n}$, for $i < j$.

Even though it is unaware of specific collaborative modes, the source is provided a codebook which allows a specific pre-determined set of time-fractions.

Each frame consisting of n bits is separated into B blocks. After receiving each block in its entirety, the relay decides if it is able to decode the data with some quality criterion (i.e. a specific BER threshold such as $BER \leq 10^{-5}$). If so, it collaborates with the source by transmitting its own blocks of parity bits for the remainder of the frame. All k information bits must be represented in the first block. Subsequent blocks can include parity bits which by themselves may not allow the possibility of decoding, but combined with previous blocks, they increase the reliability. The length of each block need not be constant. However, for simplicity, in this work we have assumed constant block length of l . Therefore, the frame length is given by $n = Bl$ and the over-all rate is $R = \frac{k}{Bl}$, regardless of the collaboration capabilities of the relay.

With constant block size, the set of time-fractions is given by

$$\Delta \in \{\frac{1}{B}, \frac{2}{B}, \dots, \frac{B-1}{B}, 1\}. \quad (3.4)$$

Figure 3.1 shows a codeword being transmitted under the three possible relay collaborative modes when $B = 3$.

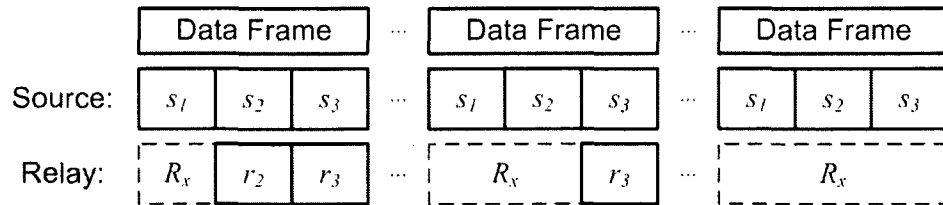


Figure 3.1. Three possible modes of collaboration when $B = 3$.

3.2.1.1 Channel Code Selection

In order to realize this transmission strategy, we can use puncturing. If we are using a block code, we set $l = k$. In the first block, the systematic bits are transmitted and we require a codebook C of rate $\frac{1}{(2-\Delta_1)B}$ such that for the case where the relay can collaborate with minimal time-fraction, all parity bits are transmitted. For any other collaborative mode, puncturing is used to determine which parity bits the relay transmits.

For a convolutional code, we have $l = k + m$, where m is the memory order of the code. The convolutional code is required to have $(2-\Delta_1)B$ outputs. The first B are used by the source, while the relay determines how many of the remaining $(1-\Delta_1)B$ it will transmit, depending on the collaborative mode (Fig. 3.2, where we have labeled each output as in Fig. 3.1).

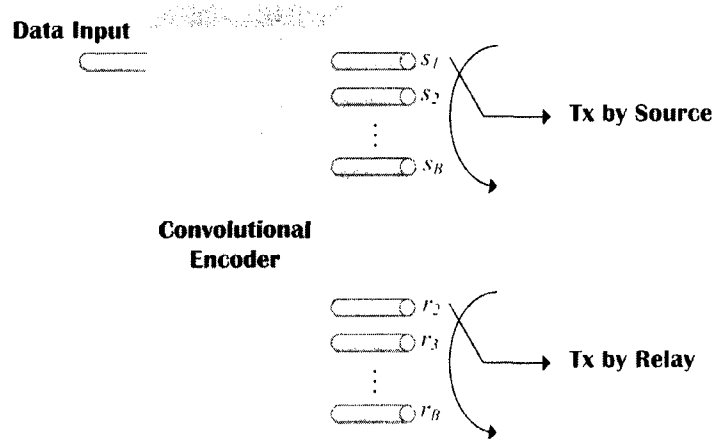


Figure 3.2. Convolutional encoder for collaborative communications.

3.2.1.2 Maximum Likelihood Decoding

At the destination, the decoder is aware of Δ and adjusts itself to take into account all of the received data. If the encoders use block codes, we can write the $2 \times Bl$ transmitted

codeword matrix as $\mathbf{V} = \begin{bmatrix} \mathbf{v}_s \\ \mathbf{v}_r \end{bmatrix} = \begin{bmatrix} \mathbf{v}_s^e & \mathbf{v}_s^c \\ \mathbf{0} & \mathbf{v}_r^c \end{bmatrix} \in \omega(C)$, where \mathbf{v}_i is the part of the codeword

transmitted by node i and $\omega(\cdot)$ is a modulation mapper. Maximum Likelihood (ML) decoding is done by selecting the codeword \mathbf{V} such that

$$|\mathbf{y}_d - \mathbf{GV}|^2 \leq |\mathbf{y}_d - \mathbf{GW}|^2, \quad (3.5)$$

for all $\mathbf{V} \neq \mathbf{W}$, $\mathbf{V}, \mathbf{W} \in \omega(C)$ and $\mathbf{y}_d = [\mathbf{y}_d^e, \mathbf{y}_d^c]$.

If the encoders use convolutional codes, the branch paths on the trellis can be labeled as $a_t / \mathbf{v}_{s,t} \mathbf{v}_{r,t}$, where a_t is the t^{th} input, $\mathbf{v}_{s,t} = (v_{s,t}, v_{s,t+l}, \dots, v_{s,t+(B-1)l})$ and $\mathbf{v}_{r,t} = (v_{r,t+\Delta Bl}, v_{r,t+(\Delta B+1)l}, \dots, v_{r,t+(B-1)l})$ are the output bits transmitted by the source and relay respectively, and where $v_{i,t}$ is the i^{th} node's output bit at time t . The ML decoder uses the Viterbi algorithm to minimize the path metric using the following branch metric equation,

$$BM_t = \sum_{b=1}^{\Delta B} \left| y_{d,t+(b-1)l}^e - G_{sd} v_{s,t+(b-1)l} \right|^2 + \sum_{b=\Delta B+1}^B \left| y_{d,t+(b-1)l}^c - G_{sd} v_{s,t+(b-1)l} - G_{rd} v_{r,t+(b-1)l} \right|^2, \quad (3.6)$$

where $1 \leq t \leq l$.

3.2.2 Decoding at the Relay

For each channel realization, a different time-fraction may be required. This time-fraction is determined at the relay and is assumed also known at the destination, either

through some header symbols or by resolving its received signal power and analyzing for a change created from s and r transmitting simultaneously.

During the first block, the relay can determine the instantaneous received SNR from the source and it can decide what Δ can be used to achieve the required reliability criterion to proceed with collaboration. The source-relay link has the following instantaneous $SNR_{s,r}$,

$$SNR_{s,r} = \gamma_{sr} |h_{sr}|^2, \quad (3.7)$$

where $\gamma_{sr} = \frac{PG_{sr}E_s}{N_o}$. Note that this SNR is not the information symbol SNR ; it is the SNR of coded/transmitted symbols.

Since each block can include error control coding, the relay is given a table providing the required $SNR_{s,r}$ thresholds, τ_{Δ_i} , for each collaborative mode, dependent on the codebook used by the source (Table 3.1).

Table 3.1. Table of thresholds for each time-fraction at the relay.

Time-Fraction Δ_i	$SNR_{s,r}$ Threshold to achieve $BER \leq 10^{-5}$
$l/n = 1/B$	τ_{Δ_1}
$2l/n = 2/B$	τ_{Δ_2}
\vdots	\vdots
$(B-1)l/n = (B-1)/B$	$\tau_{\Delta_{B-1}}$

To determine the expected value of the time-fraction, $E[\Delta]$, we must determine the probability of operating in each available collaborative mode. To maximize

collaboration, the relay always selects the minimum time-fraction that will produce $BER \leq 10^{-5}$ at the relay.

The time-fraction Δ is chosen as follows. The relay measures the $SNR_{s,r}$, and then selects the smallest Δ_i , which has $SNR_{s,r} \geq \tau_{\Delta_i}$. Or equivalently,

$$|h_{sr}|^2 \geq \frac{\tau_{\Delta_i}}{\gamma_{sr}}. \quad (3.8)$$

It is now possible to determine $E[\Delta]$ for this strategy. Since $|h_{sr}|$ is Rayleigh distributed, $\chi = |h_{sr}|^2$ is exponentially distributed with pdf $f(\chi) = e^{-\chi}$. For our chosen set of quantized time-fractions, we have,

$$E_{\chi}[\Delta] = \sum_i \Delta_i p(\Delta = \Delta_i) = \sum_{b=1}^B \frac{b}{B} p(\Delta = \frac{b}{B}), \quad (3.9)$$

where $p(\Delta = \Delta_i)$ is the probability that $\Delta = \Delta_i$. Using (3.8), we have

$$E_{\chi}[\Delta] = \sum_{b=1}^B \frac{b}{B} p\left(\frac{\tau_{b/B}}{\gamma_{sr}} \leq \chi < \frac{\tau_{(b-1)/B}}{\gamma_{sr}}\right), \quad (3.10)$$

where we have used $\tau_0 = \infty$ and $\tau_1 = 0$. Since $p(a_1 \leq \chi \leq a_2) = e^{-a_1} - e^{-a_2}$, we have

$$E_{\chi}[\Delta] = 1 - \sum_{b=1}^{B-1} \frac{1}{B} e^{-\frac{\tau_{b/B}}{\gamma_{sr}}}. \quad (3.11)$$

3.2.3 Transmitted SNR

As discussed in Section 2.4.4.1, in collaborative communications it is best to use $TSNR$ as a metric for fair comparison between different protocols. The $TSNR$ is defined as the ratio between the total transmitted signal power to the noise power at the destination.

The average $TSNR$ of the variable time-fraction collaborative protocol is given by


$$TSNR_{sr,d} = \frac{(2 - E[\Delta])^{\frac{n}{k}} E_s}{N_o}. \quad (3.12)$$

3.3 Channel Code Optimization

In this section, we provide code construction criteria which optimize the error rate performance of collaborative codes.

For modes where the relay can collaborate, we can label a frame as in Fig. 3.3, where the over-all codebook C is segmented into: C_1 corresponding to the codeword component transmitted by the source during the exchange phase, C_2 corresponding to the codeword component transmitted by the source during the collaborative phase, and C_3 corresponding to the codeword component transmitted by the relay during the collaborative phase. The length of each component depends on the specific time-fraction. The exchange phase is $n_1 = n\Delta$ symbols, while the collaborative phase is $n_2 = n(1-\Delta)$ symbols. Note that each collaborative mode has its own $C_{1,2,3} = \{C_1, C_2, C_3\}$ segmentation and as such all criteria must be satisfied for all collaborative modes. Codewords \mathbf{V} and \mathbf{W} are separated by distances d_1 , d_2 and d_3 in C_1 , C_2 and C_3 respectively. The distance can be either Hamming for binary codes or Euclidean otherwise.

Node	Exchange Phase	Collaborative Phase
Source	C_1	C_2
Relay	-----	C_3



$n_1=n\Delta$ $n_2=n(1-\Delta)$

Figure 3.3. Two-phase collaborative codes.

Neither the source nor the relay is aware of each other's location. Furthermore, we assume the location of the relay is random with uniform distribution over the plane. Therefore, code construction cannot take advantage of node topology. If the nodes were aware of each other's locations, or the location of the relay was not uniformly distributed, the channel code would be better served by a design which would take into account this knowledge. With this blindness and uniform distribution in mind, codes are constructed with the assumption that the source and relay have equal path gains to the destination. This maximizes the performance of the worst case scenario [72].

Collaborative communication is in essence a space-time code using transmitters at different locations. Therefore, to maximize the performance, we look to the rank and determinant criteria of [70]. The *PEP* is the probability of transmitting codeword matrix \mathbf{V} and deciding in favour of \mathbf{W} at the decoder. We define the Hermitian matrix $\mathbf{A}(\mathbf{V}, \mathbf{W}) = \mathbf{B}(\mathbf{V}, \mathbf{W})\mathbf{B}^\dagger(\mathbf{V}, \mathbf{W})$, where $\mathbf{B}(\mathbf{V}, \mathbf{W})$ is the codeword difference matrix

$$\mathbf{B}(\mathbf{V}, \mathbf{W}) = \begin{pmatrix} \mathbf{v}_s - \mathbf{w}_s \\ \mathbf{v}_r - \mathbf{w}_r \end{pmatrix}. \quad (3.13)$$

The rank criterion states that to maximize spatial diversity, we must ensure that $\mathbf{A}(\mathbf{V}, \mathbf{W})$ achieves full rank for all pairs of distinct codewords \mathbf{V} and \mathbf{W} . The coding criterion states that to maximize the coding gain, we must maximize the minimum of the determinant of $\mathbf{A}(\mathbf{V}, \mathbf{W})$ for all pairs of distinct codewords \mathbf{V} and \mathbf{W} .

We can now form a set of criteria to maximize the performance of variable time-fraction collaborative communication.

Criterion 1: We must maximize the performance of the worst case scenario, which is no collaboration. Since the source always transmits symbols from the same codebook, we must ensure the minimum Hamming distance of codewords in codebook $C_{1,2} = \{C_1, C_2\}$, written as $d_{1,2,\min}$ is maximized. This problem has been studied extensively [40, 45]. For higher order constellations, the minimum Euclidean distance should be maximized.

Criterion 2: For any time-fraction Δ , codewords in C_1 must contain all the information to be transmitted to the destination; otherwise it is impossible to have error-free detection at the relay. This is achieved by having a code where the minimum distance of C_1 , $d_{1,\min} > 0$. This ensures all information symbols are accounted for in the exchange phase.

Criterion 3: Since the relay is not transmitting in the first phase, we can modify $\mathbf{B}(\mathbf{V}, \mathbf{W})$,

$$\mathbf{B}(\mathbf{V}, \mathbf{W}) = \begin{pmatrix} \mathbf{v}_s^e - \mathbf{w}_s^e & \mathbf{v}_s^c - \mathbf{w}_s^c \\ \mathbf{0} & \mathbf{v}_r^c - \mathbf{w}_r^c \end{pmatrix}. \quad (3.14)$$

With $d_{1,\min} > 0$, at least one term in $(\mathbf{v}_s^e - \mathbf{w}_s^e)$ will be non-zero. In order to ensure all codeword difference matrices are of full rank – thus making all collaborative modes

achieve full diversity – one term in $\mathbf{v}_r^c - \mathbf{w}_r^c$ must be non-zero. Expressed differently, the minimum Hamming (or Euclidean) distance of C_3 is $d_{3\min} > 0$.

Criterion 4: To minimize the *PEP* of collaborative codewords, the determinant criterion [70] is used. It states that the minimum $\det \mathbf{A}(\mathbf{V}, \mathbf{W})$ for all codeword matrix pairs, must be maximized. We therefore wish to maximize the determinant of

$$\begin{aligned} \mathbf{A}(\mathbf{V}, \mathbf{W}) &= \mathbf{B}(\mathbf{V}, \mathbf{W})\mathbf{B}^\dagger(\mathbf{V}, \mathbf{W}) \\ &= \begin{bmatrix} \|\mathbf{v}_s^e - \mathbf{w}_s^e\|^2 + \|\mathbf{v}_s^c - \mathbf{w}_s^c\|^2 & (\mathbf{v}_s^c - \mathbf{w}_s^c)^H (\mathbf{v}_r^c - \mathbf{w}_r^c) \\ (\mathbf{v}_s^c - \mathbf{w}_s^c)(\mathbf{v}_r^c - \mathbf{w}_r^c)^H & \|\mathbf{v}_r^c - \mathbf{w}_r^c\|^2 \end{bmatrix}. \end{aligned} \quad (3.15)$$

For BPSK transmission, with constellation points at -1 and 1, we can further refine this criterion using the distance distribution of the codewords. By definition we have $\|\mathbf{v}_s^e - \mathbf{w}_s^e\|^2 = 4d_1$, $\|\mathbf{v}_s^c - \mathbf{w}_s^c\|^2 = 4d_2$ and $\|\mathbf{v}_r^c - \mathbf{w}_r^c\|^2 = 4d_3$. We rewrite (3.15) as

$$\begin{aligned} \mathbf{A}(\mathbf{V}, \mathbf{W}) &= \mathbf{A}_e(\mathbf{V}, \mathbf{W}) + \mathbf{A}_c(\mathbf{V}, \mathbf{W}) \\ &= \begin{bmatrix} 4d_1 & 0 \\ 0 & 0 \end{bmatrix} + \begin{bmatrix} 4d_2 & 4f \\ 4f & 4d_3 \end{bmatrix} = \begin{bmatrix} 4(d_1 + d_2) & 4f \\ & 4f & 4d_3 \end{bmatrix}, \end{aligned} \quad (3.16)$$

where $\mathbf{A}(\mathbf{V}, \mathbf{W})$ is separated into exchange phase component $\mathbf{A}_e(\mathbf{V}, \mathbf{W})$ and collaborative phase component $\mathbf{A}_c(\mathbf{V}, \mathbf{W})$. The value of f can be any negative or positive integer and is a function of the number of time slots where both the source and relay bits are in error in the collaborative phase when \mathbf{V} is transmitted and \mathbf{W} is decoded. Specifically, we have

$$f = \sum_{t=n_1+1}^n f_t, \quad (3.17)$$

where,

$$f_t = \frac{1}{4} (\mathbf{v}_{s,t} - \mathbf{w}_{s,t}) (\mathbf{v}_{r,t} - \mathbf{w}_{r,t}). \quad (3.18)$$

From the definition of f , we have the following bounds, $0 \leq |f| \leq d \Big|_{d=\min(d_1, d_2)}$.

Using the bounds on f , it is straightforward to see that the determinant of $\mathbf{A}(\mathbf{V}, \mathbf{W})$ is bounded by the following,

$$\det \mathbf{A}(\mathbf{V}, \mathbf{W}) \geq 16d_3(d_1 + d_2) - 16d^2 \Big|_{d=\min(d_2, d_3)} \quad (3.19)$$

$$\det \mathbf{A}(\mathbf{V}, \mathbf{W}) \leq 16d_3(d_1 + d_2). \quad (3.20)$$

Criterion 4.1: To maximize the minimum $\det \mathbf{A}(\mathbf{V}, \mathbf{W})$ we should minimize f .

Therefore, we should not use codes which have the source and relay transmitting the same parity symbols at the same time in the collaborative phase, since these achieve the bound of (3.19) with equality.

We look at maximizing the minimum of the determinant using block and convolutional codes.

3.3.1 Block Codes

If we use an orthogonal code, such as the Alamouti code [2], in the collaborative phase, we have $f = 0$ for all codeword pairs. Therefore, the upper bound of (3.20) is achieved with equality. We also note that the Alamouti code forces $d_3 = d_2$. Giving,

$$\mathbf{A}(\mathbf{V}, \mathbf{W}) = 16d_2(d_1 + d_2). \quad (3.21)$$

The minimum of the determinant is lower bounded by

$$\min \det \mathbf{A}(\mathbf{V}, \mathbf{W}) \geq 16d_{2\min}(d_{1,2\min}), \quad (3.22)$$

where we have used $d_1 + d_2 \geq d_{1,2\min}$. From (3.22) we see that in order to achieve the best possible coding gain when using Alamouti codes in the collaborative phase, $d_{1,2\min}$ and $d_{2\min}$ must be maximized. It is possible to take a codebook which maximizes $d_{1,2\min}$ and arrange the output bits in a way such that $d_{2\min}$ is also maximized.

We wish to determine if it is possible to construct a block code that can achieve a higher minimum determinant than one which uses an orthogonal code in the collaborative phase. In other words, we want to determine the existence of a codebook which achieves

$$16d_3(d_1 + d_2) - 16f^2 > \min \det \mathbf{A}(\mathbf{V}, \mathbf{W})|_{\text{Alamouti}} \geq 16d_{2\min}^* d_{1,2\min}^*, \quad (3.23)$$

for all codeword pairs, where d_{\min}^* is the minimum distance of a code whose minimum distance is optimized. Equation (3.23) simplifies to

$$d_3(d_1 + d_2) - d_{2\min}^* d_{1,2\min}^* > f^2 \geq 0, \quad (3.24)$$

where the last inequality comes from the fact that we don't require the code to be orthogonal.

We consider a codeword pair that has $d_1 + d_2 = d_{1,2\min}$, giving

$$d_3 d_{1,2\min} - d_{2\min}^* d_{1,2\min}^* > 0. \quad (3.25)$$

In order for this statement to be true, we must have either $d_3 > d_{2\min}^*$ or $d_{1,2\min} > d_{1,2\min}^*$.

From the definition of d_{\min}^* , it is impossible to have a strict inequality in the latter. The same argument is used for the former, since the component codewords in C_2 and C_3 have the same length.

Criterion 4.2 (Block Codes): When using block codes, it is best to use an Alamouti code in the collaborative phase since no other block code can provide a coding gain over an orthogonal code.

3.3.2 Convolutional Codes

Unlike for block codes, no orthogonal codes exist for space-time trellis (or convolutional) coding. In fact, Space-Time Trellis Codes (STTC) [70] are designed primarily to ensure full diversity, with coding gain as a secondary goal. Since from *Criterion 3* we see collaborative codes have an inherent structure that guarantees full diversity, we wish to determine if other convolutional codes provide a larger coding gain than STTCs. The lower bound on the determinant (3.19) is not a monotonic function of d_1 , d_2 and d_3 . Nevertheless, it is an increasing function.

Criterion 4.2 (Convolutional Codes): When using convolutional codes, to increase $\min \det \mathbf{A}(\mathbf{V}, \mathbf{W})$, we maximize the free distance of the codebook $C_{1,2,3} = \{C_1, C_2, C_3\}$, expressed as $d_{1,2,3\text{free}}$. This is similar to the Trace criterion given in [85].

The design of convolutional collaborative codes with variable time-fraction is done in two steps. First we select a convolutional code of rate $R = \frac{1}{(2 - \Delta_1)B}$ which maximizes $d_{1,2,3\text{free}}$. Secondly, we arrange the outputs of the convolutional encoder such that the B outputs with the highest d_{free} are used by the source and the remaining blocks are used by the relay. Special care must be taken to ensure that none of the blocks

transmitted by the source during the exchange phase are catastrophic, so that the relay can decode them.

In Table 3.2 we show convolutional codes designed for the set of time-fractions $\Delta = \{\frac{1}{3}, \frac{2}{3}, 1\}$ and satisfying all four *coding criteria*. The codes are denoted by their memory order m and are written in octal form and expressed using generator functions for each block defined in Fig. 3.1, namely $(\mathbf{g}_{s_1}, \mathbf{g}_{s_2}, \mathbf{g}_{s_3}, \mathbf{g}_{r_2}, \mathbf{g}_{r_3})_o$. The codes are in essence the best possible $R = \frac{1}{5}$ codes for different m , and have been designed using the steps described in the previous paragraph. Note that for each memory order there can be multiple channel codes that satisfy all the design criteria and as such, Table 3.2 is not exhaustive. The codes have been arranged in such a way to ensure the source has the best possible $R = \frac{1}{3}$ code (maximizing $d_{1,2\text{free}}$ from all the possible permutations of the outputs), and the source and relay don't transmit similar parity blocks at similar times in the collaborative phase. The collaborative thresholds are found by obtaining the required $SNR_{s,r}$ to achieve $BER \leq 10^{-5}$ after the relay receives either $(\mathbf{g}_{s_1})_o$ (for τ_{Δ_1}) or $(\mathbf{g}_{s_1}, \mathbf{g}_{s_2})_o$ (for τ_{Δ_2}). For relatively small frame lengths, our choice of $BER \leq 10^{-5}$ as the required criterion to assume a clear channel between the source and the relay is suitable. However, one may select a different BER criterion depending on the required performance of the source-relay link.

Table 3.2. Channel codes for variable time-fraction collaborative communications.

m	Code Generators	$d_{1,2\text{free}}$	$d_{1,2,3\text{free}}$	Collaborative Thresholds	
				τ_{Δ_1}	τ_{Δ_2}
2	$(7,5,7,7,5)_o$	8	13	9.12	2.056
3	$(15,17,15,15,17)_o$	10	16	9.12	1.709
4	$(37,27,33,25,27)_o$	10	20	9.12	1.709
5	$(75,53,47,57,65)_o$	13	22	9.12	1.333

3.4 Upper Bound on FER

In this section, we provide an analysis of the upper bound on the FER . To solve for the over-all FER , we take the conditional FER s for each collaborative mode, then average over all the possible channel coefficients. We have the following set of conditional FER s,

$$FER(G_{sd}, G_{rd}, \Delta) = \begin{cases} FER_{\Delta_1}(G_{sd}, G_{rd}) & \Delta = \Delta_1 \\ FER_{\Delta_2}(G_{sd}, G_{rd}) & \text{if } \Delta = \Delta_2 \\ \vdots & \vdots \\ FER_{\Delta_B}(G_{sd}, G_{rd}) & \Delta = \Delta_B = 1 \end{cases}. \quad (3.26)$$

Therefore, the over-all expected FER averaged over all the channel realizations is given as

$$FER = E_{G_{sr}, G_{sd}, G_{rd}} [FER(G_{sd}, G_{rd}, \Delta)] = \sum_{i=1}^B E_{G_{sd}, G_{rd}} [FER_{\Delta_i}(G_{sd}, G_{rd})] p(\Delta = \Delta_i), \quad (3.27)$$

where the probability of each time-fraction is given implicitly in (3.10).

3.4.1 Repetition Encoding

The simplest encoding strategy for collaborative communication is one where the source repeats a block of $l = k$ information bits, B times; and, when possible, the relay repeats the block until the end of the frame. This scenario achieves full diversity, but does not maximize the coding gain since *Criterion 4.1* is not met.

The conditional *BER* at the destination is given by

$$BER_{\Delta_i}(G_{sd}, G_{rd}) = Q\left(\sqrt{\frac{2BE_s}{N_o} \left[|G_{sd}|^2 \Delta_i + |G_{sd} + G_{rd}|^2 (1 - \Delta_i) \right]}\right). \quad (3.28)$$

The conditional *FER* is obtained by using the following bound,

$$FER_{\Delta_i}(G_{sd}, G_{rd}) = 1 - \left[1 - BER_{\Delta_i}(G_{sd}, G_{rd})\right]^l \leq l \cdot BER_{\Delta_i}(G_{sd}, G_{rd}). \quad (3.29)$$

The upper bound on the expected *FER* for each collaborative mode is found by averaging (3.29) over all the channel realizations,

$$E_{G_{sd}, G_{rd}}[FER_{\Delta_i}(G_{sd}, G_{rd})] \leq \int_0^\infty \int_0^\infty \int_0^{2\pi} \int_0^{2\pi} l \cdot BER_{\Delta_i}(G_{sd}, G_{rd}) \cdot pdf \cdot d|G_{sd}| d|G_{rd}| d\theta_{sd} d\theta_{rd}, \quad (3.30)$$

where for brevity we have written $pdf = pdf_{|G_{sd}|, |G_{rd}|, \theta_{sd}, \theta_{rd}}(|G_{sd}|, |G_{rd}|, \theta_{sd}, \theta_{rd})$ and since we assume all channel coefficients are independent, we have,

$$pdf(|G_{sd}|, |G_{rd}|, \theta_{sd}, \theta_{rd}) = \frac{1}{4\pi^2} \frac{4|G_{sd}||G_{rd}|}{PG_{sd}PG_{rd}} e^{-\frac{|h_{sd}|^2}{PG_{sd}}} e^{-\frac{|h_{rd}|^2}{PG_{rd}}}. \quad (3.31)$$

To get a tighter upper bound at low *SNR*, we use the limit before integration method proposed in [46] and we get

$$\begin{aligned}
& E_{G_{sd}, G_{rd}} [FER_{\Delta_i}(G_{sd}, G_{rd})] \\
& \leq \int_0^\infty \int_0^\infty \int_0^{2\pi} \int_0^{2\pi} \min(1, l \cdot BER_{\Delta_i}(G_{sd}, G_{rd})) \cdot pdf \cdot d|G_{sd}| d|G_{rd}| d\theta_{sd} d\theta_{rd}. \quad (3.32)
\end{aligned}$$

Inserting (3.32) into (3.27) lets us solve for the over-all upper bound on FER .

3.4.2 Using Channel Codes

When using channel codes, the conditional $FER_{\Delta_i}(G_{sd}, G_{rd})$ for each collaborative mode is derived using the appropriate PEP between transmitted codeword matrix \mathbf{V} and decoded codeword matrix \mathbf{W} .

The conditional $FERs$ are obtained by using an upper bound on terminated convolutional codes [37],

$$FER_{\Delta_i}(G_{sd}, G_{rd}) \leq 1 - (1 - P_{E, \Delta_i}(G_{sd}, G_{rd}))^l \leq l \cdot P_{E, \Delta_i}(G_{sd}, G_{rd}), \quad (3.33)$$

where $P_{E, \Delta_i}(G_{sd}, G_{rd})$ is the first error event probability defined as [56]

$$P_{E, \Delta_i}(G_{sd}, G_{rd}) \leq \sum_{\mathbf{d}} a_{\Delta_i}(\mathbf{d}) P_{\Delta_i}(\mathbf{d}, G_{sd}, G_{rd}), \quad (3.34)$$

where $P_{\Delta_i}(\mathbf{d}, G_{sd}, G_{rd})$ is the PEP to be defined next, $\mathbf{d} = (d_1, d_2, d_3, f)$ is the vector of distances between \mathbf{V} and \mathbf{W} . The $a_{\Delta_i}(\mathbf{d})$ are the coefficients of the weight enumerating function and can be found using standard methods [81]. Note that subscript Δ_i denotes that each mode has its own weight enumerating function, since C_1 , C_2 and C_3 represent different parts of the codewords depending on the collaborative mode.

3.4.2.1 Modified *PEP* of Collaborative Modes

Previous work on the analysis of layered codes [63] assumes that the channels from all transmit antennas differ only in small-scale fading. In collaborative communications, the source and relay have different path gains to the destination. This affects the *PEP* in (3.34). The *PEP* for any layered code, including collaborative codes, is given in (2.10) and rewritten here for clarity,

$$P_{\Delta_i}(\mathbf{d}, G_{sd}, G_{rd}) = Q \left(\sqrt{\frac{E_s}{2N_o} \|\mathbf{G}(\mathbf{V} - \mathbf{W})\|^2} \right). \quad (3.35)$$

We have,

$$\|\mathbf{G}(\mathbf{V} - \mathbf{W})\|^2 = \text{tr}(\mathbf{G}(\mathbf{V} - \mathbf{W})(\mathbf{V} - \mathbf{W})^\dagger \mathbf{G}^\dagger) = \text{tr}(\mathbf{G}\mathbf{A}(\mathbf{d})\mathbf{G}^\dagger), \quad (3.36)$$

where $\mathbf{A}(\mathbf{d}) = \mathbf{A}(\mathbf{V}, \mathbf{W})$ is given in (3.16). Equation (3.35) becomes

$$P_{\Delta_i}(\mathbf{d}, G_{sd}, G_{rd}) = Q \left(\sqrt{\frac{E_s}{2N_o} \text{tr}(\mathbf{G}\mathbf{A}(\mathbf{d})\mathbf{G}^\dagger)} \right). \quad (3.37)$$

For the case where we have no collaboration ($\Delta = 1$), we have $\mathbf{A}(\mathbf{d}) = \mathbf{A}_e(\mathbf{d})$ and the *PEP* becomes

$$P_{\Delta=1}(d_1, G_{sd}, G_{rd}) = Q \left(\sqrt{\frac{2d_1 |G_{sd}|^2 E_s}{N_o}} \right). \quad (3.38)$$

3.4.2.2 Average *FER* for Each Collaborative Mode

Similar to repetition codes, an upper bound on the expected *FER* for each collaborative mode is obtained using the limit before integration method. We have,

$$E_{G_{sd}, G_{rd}} [FER_{\Delta_i}(G_{sd}, G_{rd})] \leq \int_0^{2\pi} \int_0^{2\pi} \int_0^{\infty} \int_0^{\infty} \min \left(1, l \sum_{\mathbf{d}} a_{\Delta_i}(\mathbf{d}) P_{\Delta_i}(\mathbf{d}, G_{sd}, G_{rd}) \right) \cdot pdf \cdot d|G_{sd}| d|G_{rd}| d\theta_{sd} d\theta_{rd}, \quad (3.39)$$

and pdf is given in (3.31).

Three factors result in (3.39) being an upper bound. First, the upper bound on terminated convolutional codes of (3.33) is used. Secondly, a union upper bound is used to obtain the first error event probability of (3.34). Lastly, the bound is further loosened when we assume only the all-zero codeword is transmitted. Non-orthogonal space-time codes are not necessarily uniform, meaning the PEP is dependent on the transmitted codeword \mathbf{V} . This is seen in the definition of f , where the sum is dependent on the sign of f_i and is therefore dependent on the transmitted codeword. Any two codewords with the same Hamming distance separating them will have the same cardinality in the sum of f_i . However, if we assume the all-zero codeword is transmitted, all f_i are positive and therefore the sum of f is at a maximum. This minimizes the coding gain and yields an upper bound.

3.5 Diversity Advantage

In order to see if the protocol achieves full diversity (diversity order of 2), we need to see if FER is $O(\gamma^{-2})$, where $\gamma = \frac{E_s}{N_o}$. If the coding criteria of Section 3.3 are followed, we see that when we have collaboration, $\Delta < 1$, we achieve diversity of 2. We can separate

the terms in (3.27), into the collaborative modes ($\Delta < 1$) and the non-collaborative mode ($\Delta = 1$). We have,

$$FER = \sum_{i=1}^{B-1} FER_{\Delta_i} p(\Delta = \Delta_i) + FER_{\Delta=1} p(\Delta = 1), \quad (3.40)$$

where we have used $FER_{\Delta_i} = E_{G_{sd}, G_{rd}} [FER_{\Delta_i}(G_{sd}, G_{rd})]$.

If *criteria 2 and 3* of Section 3.3 are satisfied, the collaborative modes achieve full diversity. On the other hand, the non-collaborative mode is of diversity 1. We write

$$FER \propto p(\Delta \neq 1)O(\gamma^{-2}) + p(\Delta = 1)O(\gamma^{-1}). \quad (3.41)$$

To determine the diversity of the protocol, we wish to evaluate $p(\Delta = 1)$. From

(3.10), we have $p(\Delta = 1) = p\left(\frac{\tau_1}{\gamma_{sr}} \leq \chi \leq \frac{\tau_{B-\gamma/B}}{\gamma_{sr}}\right) = p\left(\chi \leq \frac{\tau_{B-\gamma/B}}{\gamma_{sr}}\right)$. Giving,

$$p\left(\chi \leq \frac{\tau_{B-\gamma/B}}{\gamma_{sr}}\right) = \int_0^{\frac{\tau_{B-\gamma/B}}{\gamma_{sr}}} e^{-x} dx \leq \frac{\tau_{B-\gamma/B}}{\gamma_{sr}} e^{-0} = \frac{\tau_{B-\gamma/B}}{\gamma_{sr}} \propto O(\gamma^{-1}). \quad (3.42)$$

Therefore, the second term on the right hand side of (3.41) is $O(\gamma^{-2})$ and since $p(\Delta \neq 1) \leq 1$, the first term is also at least $O(\gamma^{-2})$. The variable time-fraction protocol thus achieves full diversity at high *TSNR*, regardless of the choice of collaborative threshold $\tau_{B-\gamma/B}$. Therefore for any *BER* criterion (i.e. any set of collaborative thresholds) we will eventually reach a *TSNR* where full diversity is achieved.

3.6 Results

Unless otherwise stated, the performance results presented in this section use $B = 3$, $l = 130$, and convolutional codes of memory order m . We select $l = 130$ to keep the results presented herein consistent with the original results on Space-Time Coding presented in [70]. At high $TSNR$, modifying l would affect the over-all FER results linearly as can be seen from the bound of (3.33).

We assume blocks of equal length, the following set of time-fractions is used: $\Delta \in \{\frac{1}{3}, \frac{2}{3}, 1\}$. For adequately long frame length, we can equate a frame that is in error to an outage event. This allows us to use the outage probability as a target bound on the FER performance of collaborative communications. The outage probability of the collaborative protocol with variable time-fraction is obtained from (2.20) which is a modified version of the results of [48], in which we have added the specific effect of the respective path gains.

In Fig. 3.4 we compare the upper bound on FER , obtained from (3.27), to Monte Carlo simulations. The upper bounds are tight approximations of the simulated results to within 1 dB of $TSNR$. We also see that the variable time-fraction collaborative protocol achieves full diversity when we compare it to the outage probability. As in all results presented in this thesis, we use collaborative thresholds to achieve $BER \leq 10^{-5}$ at the relay. Modifying the BER criterion has for effect shifting the location of the curvature of the performance curve. A lower BER criterion requires larger collaborative thresholds which diminish the possibility of having high levels of collaboration at low $TSNR$. Therefore the performance exhibits unit diversity for a greater range of low $TSNR$ when

the required *BER* criterion is lowered. At high *TSNR*, a lower *BER* criterion leads to a coding loss, but not a loss in diversity.

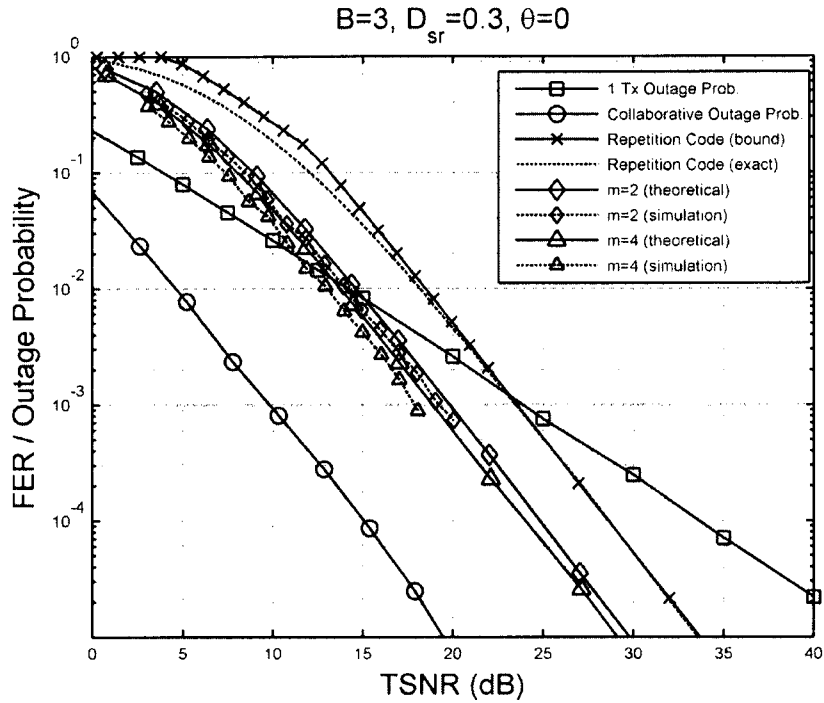


Figure 3.4. Comparison of upper bound on *FER* to simulated results for $D_{sr} = 0.3$, $\theta = 0$.

In Fig. 3.5, we compare the performance of codes of different complexity as well as traditional Space-Time Codes (STC) and the repetition code. The upper bound results all closely match the simulated results. From the upper bound results of Fig. 3.5-b), it is seen that for the same level of complexity, the best STC with $m = 2$, given by $(7,3,3,6,4)_o$ is about 1 dB weaker than the channel code selected with the highest d_{free} . Also, it is seen that using channel codes as simple as an $m = 2$ code, produces results 3.5 dB better than using the repetition code. Note however that we could use a high rate channel code

concatenated with repetition coding to improve the performance of repetition coding. However, since *Criterion 4.1* would still not be met, our proposed collaborative codes (with similar complexity) would achieve better performance.

The effect of the relay location for the $m=3$ code is shown in Fig. 3.6. The source is located at the origin and the destination is at (1,0), while the relay can be anywhere on the plane. We plot the Monte Carlo simulation results showing the required *TSNR* to achieve $FER=10^{-3}$. The best performance is obtained when $D_{sr} = 0.3$ and $\theta = 0$. Note that as expected, the results are symmetrical over the line formed by connecting the source and destination, therefore only one half is represented here for clarity. For the remainder of the thesis, results are presented only for the case where $\theta = 0$ with the understanding that with a relay placed along this axis we obtain the best possible performance of collaborative communications, as well as an overview of the general behavior. In addition, in order to standardize the results for the remainder of the thesis, when we wish to demonstrate the *FER* vs. *TSNR* relationship, we select $D_{sr} = 0.3$, since at this point the performance of collaboration is maximized. Selecting a different D_{sr} affects the numerical values of the results, but not the behavioral conclusions drawn from them.

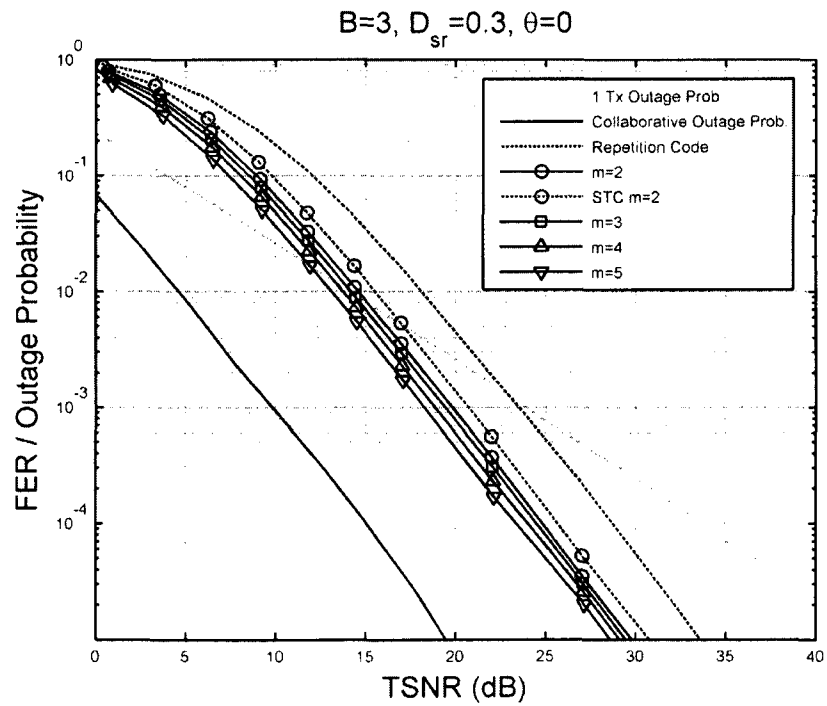
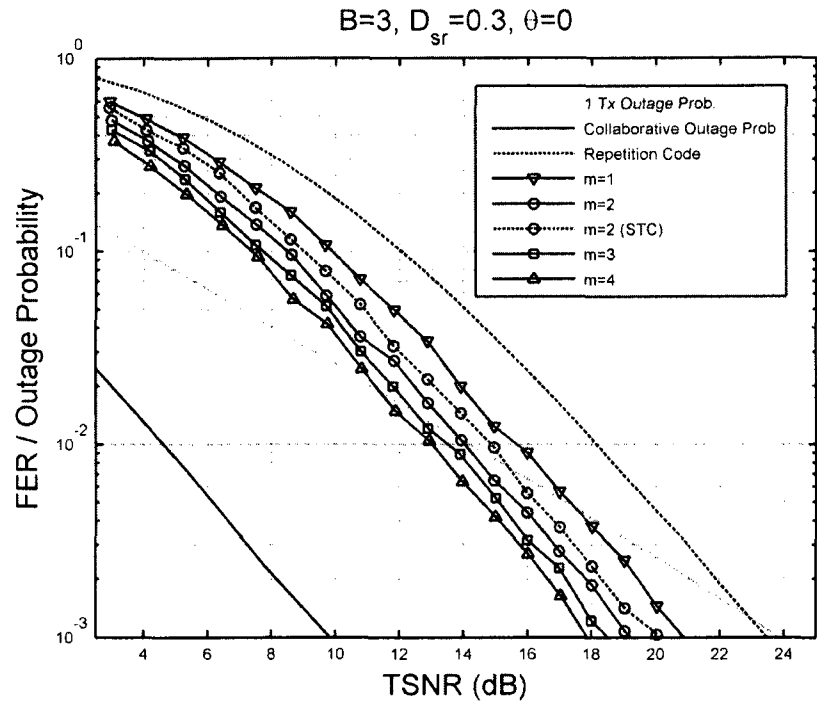


Figure 3.5. Performance of collaborative communication code with channel codes of varying complexity a) Monte Carlo simulation, b) Upper bound on FER .

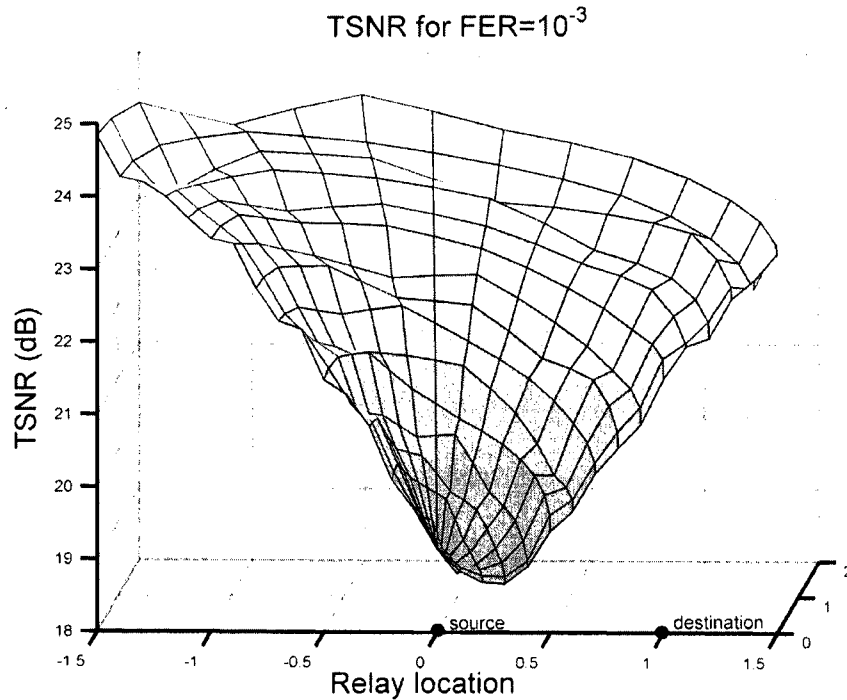


Figure 3.6. $TSNR$ required to achieve $FER=10^{-3}$ for source at origin, and destination at (1,0).

In Fig. 3.7, we further study the effect of the relay location on the required $TSNR$ to achieve a specific FER , for codes of different complexity. The results plotted here for $m = 3$ are the upper bound results of Fig. 3.6 along the one dimensional line formed by joining the location of the source and destination. We compare the performance of codes with different complexity. The source is located at the origin, while the destination is located at a normalized distance of 1. Although not provided graphically in this thesis, results (including those of Fig. 3.6) show that for all relay locations plotted in Fig. 3.7, all the codes provide full diversity. Using the FER upper bound, we have plotted the $TSNR$ required to achieve a FER of 10^{-3} at the destination. We see that for any code

complexity, the lowest required $TSNR$ is achieved with a relay located around $D_{sr} = 0.3$. For a relay located any closer to the destination, the ability to collaborate will be diminished since PG_{sr} will be decreased. On the other hand, a relay located any closer to the source will lead to a poorer (r,d) channel. As seen in Fig. 3.5, the non-collaborative outage probability is 23.5 dB for $FER = 10^{-3}$. Therefore even for the simple code with $m=2$ and with relay located beyond the destination, as far as $D_{sr} = 1.25$, the variable time-fraction collaborative protocol shows a gain over strict non-collaboration.

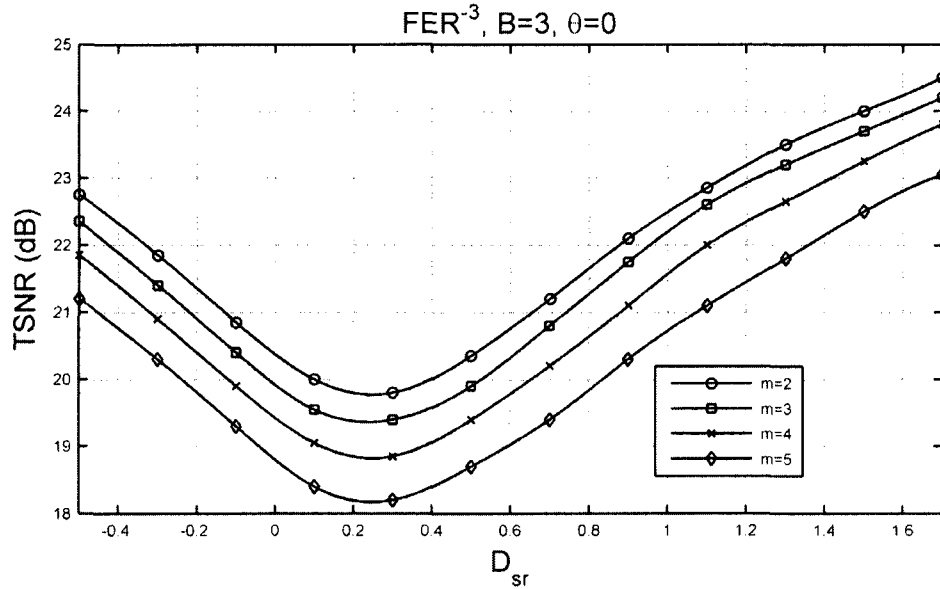
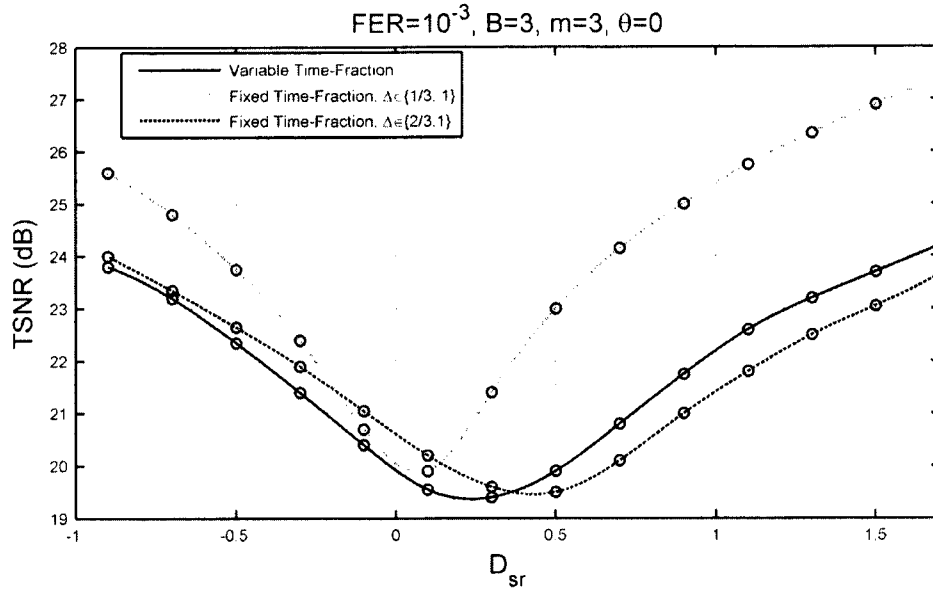


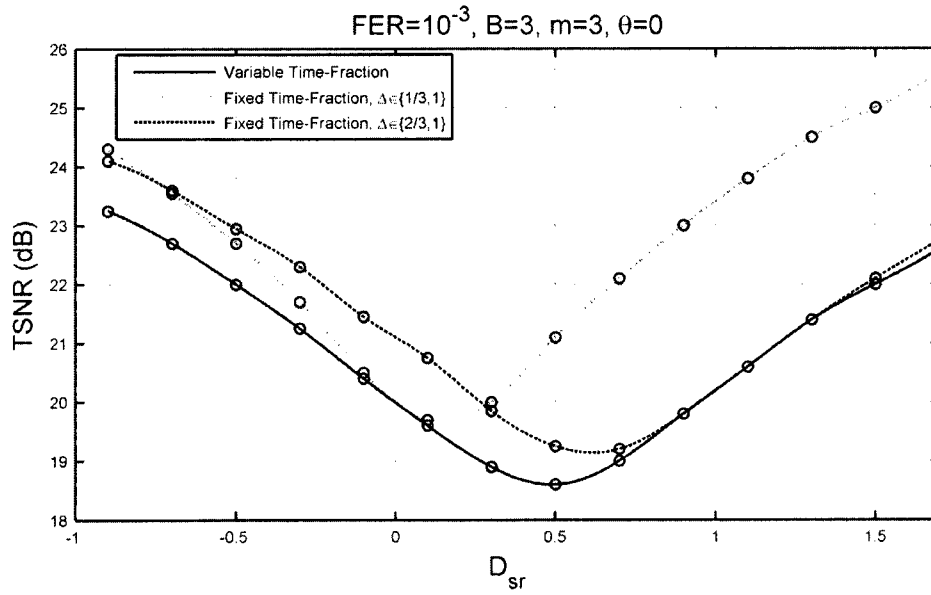
Figure 3.7. FER performance with source at origin and destination at 1, $\theta = 0$.

In order to validate the use of a variable time-fraction, in Fig. 3.8, we have compared the performance of a variable time-fraction protocol to ones with fixed time-fractions. We characterize a protocol as fixed time-fraction when Δ can take one of two

values: Δ_1 when collaboration is possible, or 1 if it is not. We define a fixed time-fraction 1/3 protocol to have $\Delta \in \{\frac{1}{3}, 1\}$, and a fixed time-fraction 2/3 protocol to have $\Delta \in \{\frac{2}{3}, 1\}$. In Fig. 3.8-a) we see that the variable time-fraction protocol always outperforms the 1/3 protocol. When the relay moves away from s towards d , the 2/3 protocol achieves better performance than the variable time-fraction protocol. This is because the variable time-fraction protocol lowers the $E[\Delta]$ since there are scenarios where the relay will transmit two blocks, while the 2/3 protocol never has these scenarios. In order to compare the two protocols, the *TSNR* of both protocols must be equal. Normalizing the *TSNR* of the two protocols requires a reduction of E_s in the variable time-fraction protocol. This affects all collaborative modes, and since only one mode benefits from having the relay transmit 2 blocks, the over-all effect is a loss in performance. This can be remedied by adding a simple feedback from the relay or destination to the source informing it of when the relay can collaborate. Such a scheme requires $\lceil \log_2 B \rceil$ bits of feedback. During the collaborative phase, the source and relay transmit with $\frac{1}{2} E_s$. Because the total transmitted signal power is constant, the *TSNR* is no longer a function of $E[\Delta]$. Figure 3.8-b) shows results for the feedback scheme. We see that for situations where $D_{sr} < 0.7$, the variable time-fraction will outperform even an “optimal” choice of the best fixed time-fraction protocol. On the other hand, when $D_{sr} \geq 0.7$, the variable time-fraction protocol’s performance equals that of the 2/3 protocol. The improvement obtained from using a variable time-fraction protocol is expected since for the same *TSNR*, the variable time-fraction protocol provides more



a)



b)

Figure 3.8. Comparison of fixed time-fraction to variable time-fraction for a) Source without feedback, b) Source with simple feedback allowing for constant transmitted power.

collaborative possibilities. Using the simple feedback to make *TSNR* constant improves the performance for both fixed and variable time-fraction protocols. That is because

there is no longer an increase in $TSNR$ associated with an increase in collaboration. These results demonstrate the versatility of using a variable time-fraction protocol, since the relay does not require knowledge of its position to decide which fixed time-fraction to use.

3.7 Conclusion

In this chapter we have proposed a general collaborative strategy that achieves full diversity using DF. In this strategy, the source transmits for the duration of the frame, while the relay listens for a variable amount of time until it can decode with a certain quality, at which point it begins collaboration. The proposed collaborative communication strategy is flexible and can accommodate scenarios as simple as ones where the source is effectively blind to all channel characteristics. We have developed rules for the implementation of the protocol, such as the determination of the time-fraction at the relay. We have also proposed channel code design criteria to maximize the performance. Using the proposed analysis tools (that are applicable for any binary layered codes), we have derived an upper bound on the FER of variable time-fraction collaborative communications. Variable time-fraction collaboration is shown to provide full diversity advantage. The coding criteria are shown to be effective in building strong collaborative channel codes that outperform the use of STC in the collaborative phase. Variable time-fraction is also shown to outperform fixed time-fraction protocols for all locations of the relay when using a simple feedback.

CHAPTER 4

Effect of Imperfect *CSIR* on Variable Time-Fraction Collaborative Communications

4.1 Introduction

For soft-decision maximum-likelihood decoding, *CSIR* is required. Having perfect *CSIR* is purely hypothetical, since the receivers need to estimate the channel parameters. In this chapter we investigate the effect of having imperfect *CSIR* at both the relay and destination, on the performance of variable time-fraction collaborative communications.

This problem was previously investigated for different communication systems [13, 29, 54, 67, 89, 90]. However, previous work on collaboration has assumed perfect *CSIR* at the relay and destination. In collaboration, the effect of imperfect *CSIR* is

twofold: the ability of the relaying node to collaborate is affected, as is the performance of the decoder at the destination.

The results obtained in this chapter are applicable to any estimation technique, as well as to any collaborative communication protocol. We present an analytical framework to study the effect of imperfect *CSIR* which takes into consideration the node locations. Next, we obtain results that show the effect of imperfect *CSIR* at the relay can be taken into account by modifying the thresholds used to determine the collaborative mode. By analyzing the *PEP*, we also show the effect of imperfect *CSIR* on the over-all *FER* of collaborative communications. The use of Pilot Symbol Assisted Modulation (*PSAM*) to estimate the channel coefficients is investigated. We further obtain the optimal number of pilot symbols, which optimizes the error performance of collaborative communication in quasi-static fading channels. The results show that imperfect *CSIR* affects the coding gain of collaborative communications, but not the diversity advantage. We also show that the optimal number of pilot symbols is not affected by the channel code used or by the location of the relay, for practical relay locations.

The chapter is organized as follows; in Section 4.2 we provide a system model altered from that of Chapter 3 to better articulate the effect of imperfect *CSIR*. Section 4.3 we discuss the effect of estimating the channel coefficients. In Section 4.4 we provide an analysis of the *PEP* of variable time-fraction collaborative communication with imperfect *CSIR*. Section 4.5 discusses using *PSAM* to obtain channel coefficient estimates. In Section 4.6 we provide an analysis of the optimal number of pilot symbols for *PSAM*. Section 4.7 provides some results and Section 4.8 gives concluding remarks.

4.2 System Model

We will see in this chapter that the effect of imperfect *CSIR* depends on the number of channels from which the destination receives signals. In short, the estimation at the destination is compounded as more signals are received simultaneously through different channels. Because of this we rewrite the *PEP* in (3.35) as

$$P_{\Delta}(\mathbf{d}, \mathbf{G}) = Q\left(\sqrt{\gamma_e + \gamma_c}\right), \quad (4.1)$$

where γ_e represents the contribution from the exchange phase and γ_c represents the contribution from the collaborative phase. We can separate the contribution from the two phases since they are affected by independent noise samples due to the signals being transmitted at different times. We have,

$$\gamma_e = \frac{E_s}{2N_o} \text{tr}\left(\mathbf{G}\mathbf{A}_e(\mathbf{d})\mathbf{G}^\dagger\right) = \frac{2E_s}{N_o} |G_{sd}|^2 d_1, \quad (4.2)$$

and

$$\gamma_c = \frac{E_s}{2N_o} \text{tr}\left(\mathbf{G}\mathbf{A}_c(\mathbf{d})\mathbf{G}^\dagger\right). \quad (4.3)$$

Note that for the case when the relay cannot collaborate, $\Delta = 1$ and $\gamma_c = 0$.

4.3 Effect of Imperfect *CSIR*

The use of *CSIR* is necessary in this protocol. At the relay and destination, *CSIR* is used to decide on the time-fraction as well as for decoding of the data.

The results obtained in Chapter 3 require perfect knowledge of *CSIR*. This assumption is not practically achievable since the channel coefficients are estimated at both the relay and destination. In this Chapter, we assume a more practical scenario where the relay and destination obtain possibly erroneous estimates on the channel coefficients \hat{G}_{sr} at the relay and $\hat{\mathbf{G}} = (\hat{G}_{sd}, \hat{G}_{rd})$ at the destination. If the wireless nodes are considered immobile, the path gain will not vary between each frame. It can therefore be surmised that the path gain can be estimated without error. In such a case we only have to estimate the fading coefficients. However, since at the receivers we only care for the full channel coefficients (and not its constituent path gain and fading coefficient), the performance of the decoder does not change whether we assume perfect knowledge of path gains with the need to estimate fading coefficients, or the need to estimate the full channel coefficients.

We assume that the entries of \hat{G}_{sr} and $\hat{\mathbf{G}}$ are i.i.d. zero-mean complex Gaussian random variables.

First we solve for the case of having estimates for two channel coefficients for a layered code, such as is the case at the destination during the collaborative phase. The simpler case of obtaining the error performance with one estimated channel coefficient (such as the estimate of G_{sr} at the relay, or during the exchange phase at the destination) is basically a simplified version of having two estimated channel coefficients, and is given in [29]. The performance of the collaborative phase is effectively a 2x1 MISO scheme. However, this can be easily extended to higher order MIMO channels with varying path gains. We let ρ_{ij} denote the correlation coefficient between G_{ij} and \hat{G}_{ij} .

Also let $\zeta_{ij} = \text{var}(G_{ij}) / \text{var}(\hat{G}_{ij})$ denote the power ratio between G_{ij} and \hat{G}_{ij} . Following the model of [29], we have

$$\mathbf{G} = \hat{\mathbf{G}}\mathbf{Y} + \Xi, \quad (4.4)$$

where

$$\begin{aligned} \mathbf{Y} &= \begin{bmatrix} Y_{sd} & 0 \\ 0 & Y_{rd} \end{bmatrix} = \begin{bmatrix} \sqrt{\zeta_{sd}} \rho_{sd} & 0 \\ 0 & \sqrt{\zeta_{rd}} \rho_{rd} \end{bmatrix} \\ &= \begin{bmatrix} \sqrt{\zeta_{sd}} & 0 \\ 0 & \sqrt{\zeta_{rd}} \end{bmatrix} \begin{bmatrix} \rho_{sd} & 0 \\ 0 & \rho_{rd} \end{bmatrix} = \bar{\zeta}^{1/2} \bar{\rho} \end{aligned}, \quad (4.5)$$

and Ξ is the 1x2 estimation error matrix, independent of $\hat{\mathbf{G}}$. The entries of Ξ are also i.i.d. zero-mean complex Gaussian random variables. The covariance matrix of Ξ is

$$\mathbf{Q} = \begin{bmatrix} PG_{sd}(1-\rho_{sd}^2) & 0 \\ 0 & PG_{rd}(1-\rho_{rd}^2) \end{bmatrix}. \quad (4.6)$$

The model is general; specific values of ρ_i and ζ_i depend on the specific channel estimation technique employed.

We wish to find the probability of receiving a specific signal at time t , given the transmitted signal and the estimate on the channel,

$$\begin{aligned} p(y_{d,t}^c | \mathbf{X}_t^c, \hat{\mathbf{G}}) &= E_{\Xi} \left[p(y_{d,t}^c | \mathbf{X}_t^c, \hat{\mathbf{G}}, \Xi) \right] \\ &= \frac{1}{(\pi N_o)} E_{\Xi} \left[\exp \left\{ \frac{-E_s}{N_o} \left\| y_{d,t}^c - \hat{\mathbf{G}}\mathbf{Y}\mathbf{X}_t^c - \Xi\mathbf{X}_t^c \right\|^2 \right\} \right] \end{aligned} \quad (4.7)$$

It is shown in [29] that (4.7) can be rewritten as

$$p(y_{d,t}^c | \mathbf{X}_t^c, \hat{\mathbf{G}}) = \frac{1}{(\pi N_o) |\Omega|} \exp \left\{ -tr(\Theta^\dagger \Psi \Theta) \right\}, \quad (4.8)$$

where

$$\Theta = \sqrt{E_s} \hat{\mathbf{G}} \Upsilon \mathbf{X}_t^c - y_t^d, \quad (4.9)$$

$$\Omega = 1 + \frac{E_s}{N_o} (\mathbf{X}_t^c)^\dagger \mathbf{Q} \mathbf{X}_t^c, \quad (4.10)$$

$$\Psi = \left(E_s (\mathbf{X}_t^c)^\dagger \mathbf{Q} \mathbf{X}_t^c \right)^{-1} [1 - \Omega^{-1}]. \quad (4.11)$$

Hence, $(y_{d,t}^c | \mathbf{X}_t^c, \hat{\mathbf{G}})$ is a random variable with distribution $\mathcal{C}(\sqrt{E_s} \hat{\mathbf{G}} \Upsilon \mathbf{X}_t^c, N_o + \text{tr}(\mathbf{Q}) E_s)$.

4.4 PEP with Imperfect CSIR

4.4.1 Decoding at the Relay with Imperfect CSIR

When decoding at the relay with imperfect CSIR, we use \hat{G}_{sr} instead of $\hat{\mathbf{G}}$, $\Upsilon_{sr} = \sqrt{\zeta_{sr}} \rho_{sr}$ instead of Υ and $Q_{sr} = P G_{sr} (1 - \rho_{sr}^2)$ instead of \mathbf{Q} . The PEP for a simple SISO link with imperfect CSIR is obtained by modifying the classical PEP to have mean $\sqrt{E_s} \hat{G}_{sr} \sqrt{\zeta_{sr}} \rho_{sr} x_{s,t}^e$ and complex variance $N_o + P G_{sr} (1 - \rho_{sr}^2) E_s$. We have,

$$\begin{aligned} P_{\text{relay}}(d_1, \hat{G}_{sr}) &= Q \left(\sqrt{\frac{2E_s d_1}{(N_o + P G_{sr} (1 - \rho_{sr}^2) E_s)}} \hat{G}_{sr} \Upsilon_{sr} \Upsilon_{sr}^\dagger \hat{G}_{sr}^\dagger \right) \\ &= Q \left(\sqrt{\frac{2E_s d_1 \rho_{sr}^2}{(N_o + P G_{sr} (1 - \rho_{sr}^2) E_s)}} \hat{G}_{sr} \sqrt{\zeta_{sr}} (\hat{G}_{sr} \sqrt{\zeta_{sr}})^\dagger \right) \end{aligned}$$

Rewritten, we have,

$$P_{relay}(d_1, \tilde{G}_{sr}) = Q \left(\sqrt{\frac{2E_s d_1 \rho_{sr}^2}{(N_o + PG_{sr}(1 - \rho_{sr}^2)E_s)} |\tilde{G}_{sr}|^2} \right), \quad (4.12)$$

where $\tilde{G}_{sr} = \sqrt{\zeta_{sr}} \hat{G}_{sr}$ is identically distributed as G_{sr} and d_1 is defined in Chapter 3.

Comparing (4.12) to the classical *PEP* of (2.6), we see that with imperfect *CSIR* at the relay, we have a coding loss of

$$10 \log \left[\frac{\rho_{sr}^2}{1 + PG_{sr} \left(1 - \rho_{sr}^2\right) \frac{E_s}{N_o}} \right]^{-1} \text{ dB}. \quad (4.13)$$

In order to evaluate (3.27) with imperfect *CSIR*, we need to evaluate the probability of each time-fraction. This probability is dependent on the performance of decoding at the relay. Using the coding loss of (4.13), we can generate a new set of thresholds for a system with imperfect *CSIR*. We denote the new thresholds as τ'_{Δ_i} , and we have

$$\tau_{\Delta_i} = \left[\frac{\rho_{sr}^2}{1 + PG_{sr} \left(1 - \rho_{sr}^2\right) \tau'_{\Delta_i}} \right] \tau'_{\Delta_i},$$

giving

$$\tau'_{\Delta_i} = \frac{\tau_{\Delta_i}}{\rho_{sr}^2 (1 + PG_{sr} \tau_{\Delta_i}) - PG_{sr} \tau_{\Delta_i}}. \quad (4.14)$$

4.4.2 Decoding at the Destination with Imperfect *CSIR*

The coding loss seen at the receiver of the destination affects the two phases of collaborative communications differently. This is dependent on the number of channel

coefficients being estimated in each phase. In this case, the *PEP* of (4.1) becomes dependent on the estimated channel coefficients, $P_{\Delta_i}(\mathbf{d}, \hat{\mathbf{G}})$, and γ_e and γ_c become

$$\gamma_e = \frac{E_s}{2(N_o + PG_{sd}(1 - \rho_{sd}^2)E_s)} \text{tr}(\hat{\mathbf{G}}\Upsilon\mathbf{A}_e(\mathbf{d})\Upsilon^\dagger\hat{\mathbf{G}}^\dagger), \quad (4.15)$$

and

$$\gamma_c = \frac{E_s}{2(N_o + (PG_{sd}(1 - \rho_{sd}^2) - PG_{rd}(1 - \rho_{rd}^2))E_s)} \text{tr}(\hat{\mathbf{G}}\Upsilon\mathbf{A}_c(\mathbf{d})\Upsilon^\dagger\hat{\mathbf{G}}^\dagger). \quad (4.16)$$

Using the same arguments as in (4.12), we have

$$\gamma_e = \frac{E_s}{2(N_o + PG_{sd}(1 - \rho_{sd}^2)E_s)} 4d_1\rho_{sd}^2 |\tilde{G}_{sd}|^2. \quad (4.17)$$

For γ_c we have,

$$\begin{aligned} \gamma_c &= \frac{E_s}{2(N_o + (PG_{sd}(1 - \rho_{sd}^2) - PG_{rd}(1 - \rho_{rd}^2))E_s)} \text{tr}(\hat{\mathbf{G}}\sqrt{\zeta}\bar{\rho}\mathbf{A}_c(\mathbf{d})\bar{\rho}^\dagger\sqrt{\zeta}^\dagger\hat{\mathbf{G}}^\dagger) \\ &= \frac{E_s}{2(N_o + (PG_{sd}(1 - \rho_{sd}^2) - PG_{rd}(1 - \rho_{rd}^2))E_s)} \text{tr}(\tilde{\mathbf{G}}\bar{\rho}\mathbf{A}_c(\mathbf{d})\bar{\rho}^\dagger\tilde{\mathbf{G}}^\dagger) \end{aligned} \quad (4.18)$$

where $\tilde{\mathbf{G}} = \zeta^{1/2}\hat{\mathbf{G}}$ is identically distributed as \mathbf{G} .

To solve for the *FER*, the values obtained in (4.17) and (4.18) are used in (4.1), which in turn is used in (3.27) and (3.39), where in (3.27) the expectation is done over \tilde{G}_{sr} , \tilde{G}_{sd} and \tilde{G}_{rd} .

4.5 Using Pilot Symbol Assisted Modulation

One method to obtain estimates of the channel coefficients is to use *PSAM*. The channel estimates are obtained by transmitting a pilot sequence of length n_p for each link [69, 89]. The received signal at the destination during the pilot symbol transmission is given by

$$\mathbf{y}_d^p = \sqrt{E_p} \mathbf{G} \mathbf{X}^p + \mathbf{z}_d^p, \quad (4.19)$$

where \mathbf{y}_d^p and \mathbf{z}_d^p are $1 \times n_p$ vectors, E_p is the energy of each pilot symbol and $\mathbf{X}^p = [\mathbf{x}_{sd}^p, \mathbf{x}_{rd}^p]^T$ denotes the $2 \times n_p$ matrix of pilot symbols. We assume the pilot sequences for each link are orthogonal. This means that the relay can properly estimate the pilot sequence obtained from the source in a similar method that is detailed here for the destination.

The maximum likelihood (ML) estimates of the fading coefficients is given by

$$\hat{G}_{ij} = \frac{\mathbf{y}_d^p (\mathbf{x}_{ij}^p)^\dagger}{\sqrt{E_p n_p}} = G_{ij} + \frac{\mathbf{z}_d^p (\mathbf{x}_{ij}^p)^\dagger}{\sqrt{E_p n_p}} = G_{ij} + e_{ij}, \quad (4.20)$$

where e_{ij} is the estimation error and we have used $\|\mathbf{x}_{ij}^p\|^2 = n_p$. The estimation error is $e_{ij} \sim \mathcal{C}(0, \sigma_{e_{ij}}^2)$ with complex variance,

$$\sigma_{e_{ij}}^2 = \frac{N_o}{n_p E_p}. \quad (4.21)$$

We can now solve for the correlation coefficients in terms of the complex variance of the estimation error,

used per frame. Therefore, as we increase the amount of energy used by the pilot symbols, we in effect decrease the amount of energy available for the transmission of data.

In this section, we study the optimal number of pilot symbols to minimize the over-all *FER* at the destination.

We can rewrite (4.1) as

$$P_{\Delta_i}(\mathbf{d}, \tilde{\mathbf{G}}) = Q\left(\sqrt{\gamma_e^{\text{gain}} \gamma_e^{\text{perfect}} + \gamma_c^{\text{gain}} \gamma_c^{\text{perfect}}}\right), \quad (4.24)$$

where $\gamma_e^{\text{perfect}}$ and $\gamma_c^{\text{perfect}}$, given in (4.2) and (4.3) respectively, represent the values of γ_e and γ_c with perfect *CSIR*, and γ_e^{gain} and γ_c^{gain} represent the effect of imperfect *CSIR* on each component of the *PEP*.

We wish to obtain the individual γ_e^{gain} and γ_c^{gain} for each collaborative mode. From these, we obtain the optimal number of pilot symbols for each collaborative mode and then select a compromise for over-all communication. If for perfect *CSIR* – requiring no estimation – the energy per symbol is given as E_s^{perfect} , then for each collaborative mode, the energy for non-pilot symbols with imperfect *CSIR* is given by

$$E_s = \alpha_{\Delta_i} E_s^{\text{perfect}}, \quad (4.25)$$

where $\alpha_{\Delta_i} = \frac{2n - n\Delta_i}{2n - n\Delta_i + 2n_p \delta}$, and $n = Bl$ is the length of encoded data in each frame.

Comparing (4.17) to (4.2) we get

$$\gamma_e^{\text{gain}} = \frac{\alpha_{\Delta_i} \rho_{sd}^2}{1 + PG_{sd}(1 - \rho_{sd}^2)\alpha_{\Delta_i} \gamma} \approx \frac{\delta n_p \alpha_{\Delta_i}}{\delta n_p + 1}, \quad (4.26)$$

where we have used (4.22) and $\gamma = \frac{E_s^{perfect}}{N_o}$ and the rightmost term in (4.26) is valid for medium to high γ . If we integrate (4.26) over n_p and set to zero, we can find the optimal number of pilot symbols, to maximize γ_e^{gain} for each collaborative mode,

$$n_p^{opt} = \sqrt{\frac{(2n - n\Delta_i)}{2\delta^2}}. \quad (4.27)$$

The analysis is slightly more complicated for the γ_c^{gain} term. The numerator of γ_c in (4.18) can be written as

$$\begin{aligned} E_s \tilde{\mathbf{G}} \bar{\rho} \mathbf{A}_c(\mathbf{d}) \bar{\rho}^\dagger \tilde{\mathbf{G}}^\dagger &= E_s \tilde{\mathbf{G}} \begin{bmatrix} \rho_{sd}^2 d_2 & \rho_{sd} \rho_{rd} f \\ \rho_{sd} \rho_{rd} f & \rho_{rd}^2 d_3 \end{bmatrix} \tilde{\mathbf{G}}^\dagger \\ &= E_s |\tilde{\mathbf{G}}_{sd}|^2 \rho_{sd}^2 d_2 + E_s \tilde{\mathbf{G}}_{sd} \tilde{\mathbf{G}}_{rd}^\dagger \rho_{sd} \rho_{rd} f + E_s \tilde{\mathbf{G}}_{sd}^\dagger \tilde{\mathbf{G}}_{rd} \rho_{sd} \rho_{rd} f + E_s |\tilde{\mathbf{G}}_{rd}|^2 \rho_{rd}^2 d_3 \end{aligned}$$

Therefore, when comparing (4.18) to (4.3), we can split the γ_c term into three separate terms, each with its own γ_c^{gain} given by

$$\gamma_c^{gain(1)} = \frac{\alpha_{\Delta_i} \rho_{sd}^2}{1 + \left(PG_{sd} (1 - \rho_{sd}^2) + PG_{rd} (1 - \rho_{rd}^2) \right) \alpha_{\Delta_i} \gamma}, \quad (4.28)$$

$$\gamma_c^{gain(2)} = \frac{\alpha_{\Delta_i} \rho_{sd} \rho_{rd}}{1 + \left(PG_{sd} (1 - \rho_{sd}^2) + PG_{rd} (1 - \rho_{rd}^2) \right) \alpha_{\Delta_i} \gamma}, \quad (4.29)$$

$$\gamma_c^{gain(3)} = \frac{\alpha_{\Delta_i} \rho_{rd}^2}{1 + \left(PG_{sd} (1 - \rho_{sd}^2) + PG_{rd} (1 - \rho_{rd}^2) \right) \alpha_{\Delta_i} \gamma}. \quad (4.30)$$

At medium to high γ , all three gain factors are approximated by

$$\gamma_c^{gain} \approx \frac{\delta n_p \alpha_{\Delta_i}}{\delta n_p + 2}. \quad (4.31)$$

From (4.31), we can find the optimal number of pilot symbols to maximize γ_c^{gain} ,

because there are fewer cases where both the source and the relay transmit concurrently; such modes require a greater number of pilot symbols. The same can be said of protocols such as selection relaying and coded cooperation, where there are no modes where the source and relay transmit data concurrently. Note that an effective fractional number of pilot symbols can be achieved by varying the energy of the pilot symbols.

Table 4.1. Optimal number of pilot symbols.

Collaborative Protocol	Optimal number of pilot symbols	As a percentage of the frame length
Variable Time-Fraction protocol $\Delta = \{\frac{1}{3}, \frac{2}{3}, 1\}$, $n = 390$	19.28	9.89%
Variable Time-Fraction protocol $\Delta = \{\frac{1}{3}, \frac{2}{3}, 1\}$, $n = 600$	23.92	7.97%
Variable Time-Fraction protocol $\Delta = \{\frac{1}{2}, 1\}$, $n = 390$	18.42	9.45%
Selection Relaying protocol [44] $\Delta = \{\frac{1}{2}, 1\}$, $n = 390$	13.96	7.16%
Coded Cooperation protocol [30] $\Delta = \{\frac{1}{2}, 1\}$, $n = 390$	11.92	6.11%

4.7 Results

The results presented in this section use $B = 3$, $l = 130$ as well as the following set of time-fractions, $\Delta \in \{\frac{1}{3}, \frac{2}{3}, 1\}$. The channel code used for the results is the $m = 3$ code with generator matrix $(15, 17, 15, 15, 17)_0$.

With the relay located at $D_{sr} = 0.3$ and $\theta = 0$, in Fig. 4.1 we study the effect of having imperfect *CSIR*. As expected, increasing the number of pilot symbols in *PSAM* improves the *FER* performance, up to $n_p = 20$. Using *PSAM* with $n_p = 1$ leads to a loss of about 4 dB versus perfect *CSIR* at the relay and destination; while *PSAM* with $n_p = 20$ only produces a loss of about 0.6 dB. The loss is due to a combination of having some decoding errors created due to the imperfect *CSIR* at the destination, as well as requiring higher *SNR* thresholds at the relay to achieve collaboration. Note that even for $n_p = 1$, the *FER* performance shows the same diversity advantage as obtained with perfect *CSIR*.

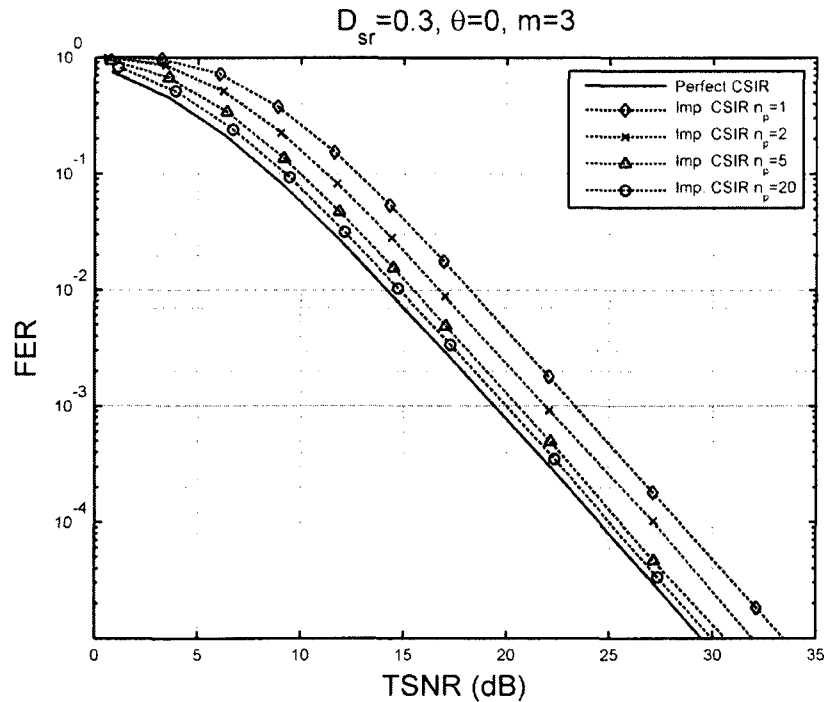


Figure 4.1. *FER* with imperfect *CSIR* and varying number of pilot symbols for $D_{sr} = 0.3$ and $\theta = 0$.

$$F^C(Z_I, Z_{II}, Z_{III}) = \sum_{d_I} Z_I^{d_I} F_{d_I}^C(Z_{II}, Z_{III}). \quad (5.43)$$

Note that to obtain the coefficients for all time-fractions we use the following distance designation,

- for $\Delta = \frac{1}{3}$: $d_1 = d_I$ and $d_2 = d_{II} + d_{III}$
- for $\Delta = \frac{2}{3}$: $d_1 = d_I + d_{II}$ and $d_2 = d_{III}$
- for $\Delta = 1$: $d_1 = d_I + d_{II} + d_{III}$.

5.6.1 Results

The turbo code results are obtained by using the same constituent encoder for both encoder a and b in Fig. 5.6, namely the $m=2$ convolutional code $(1,7)_6$. The results of Fig. 5.7 show that using a simple Turbo code can result in a variable time-fraction collaborative code whose performance is basically equivalent to the $m=5$ convolutional variable time-fraction collaborative code. This is true for both *OPAA* and *SPAA*. The results show that the loss in collaborative capabilities - due to a weaker code being used in the exchange phase for the Turbo coded system - are overcome by the gains provided by the Turbo coding principle and more specifically the uniform interleaver.

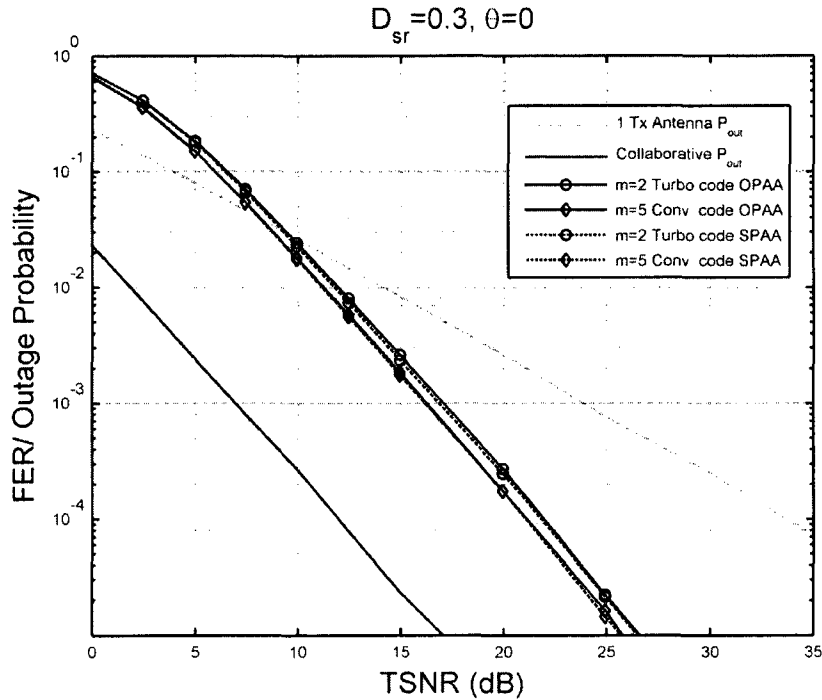


Figure 5.7. *FER* performance of Turbo coded variable time-fraction collaborative communications.

In Fig. 5.8, we see the required *TSNR* to achieve $FER=10^{-3}$ for different relay locations. We note that for all relay locations, when using the *OPAA*, the turbo coded variable time-fraction collaborative code performs similar to the $m = 5$ convolutional variable time-fraction collaborative code. On the other hand for the *SPAA* the performance is always within 0.2 dB. The difference in collaborative capabilities, due to different collaborative thresholds, is felt more in the *SPAA* especially when the relay is near the source. Nevertheless, the results show that with simple constituent codes, Turbo coded variable time-fraction collaborative communication has strong performance for all relay locations.

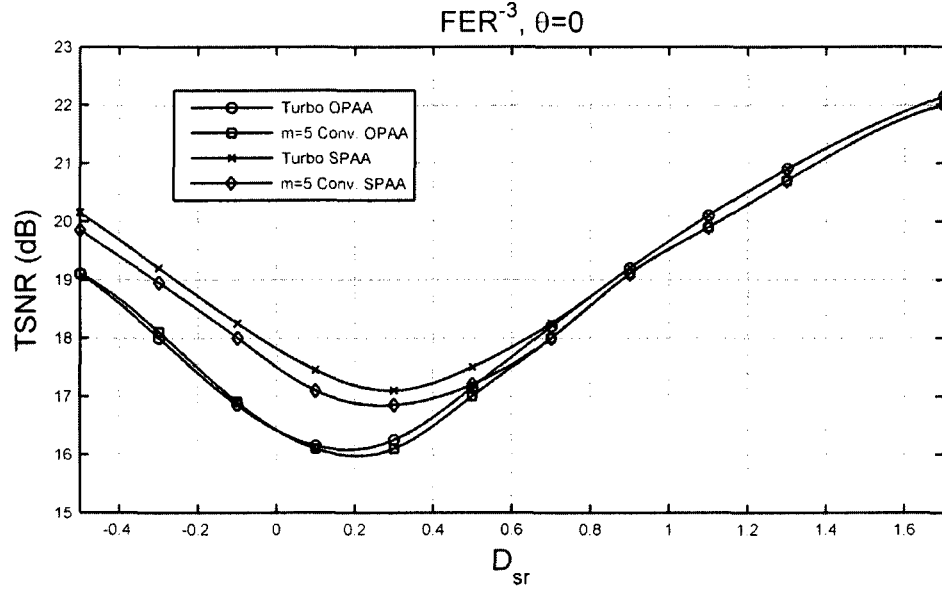


Figure 5.8. Comparison of Turbo coded collaboration to convolutionally encoded collaboration for different *PAA* algorithms, and for varying relay locations, with the source at the origin, the destination at 1 and $\theta = 0$.

5.7 Conclusion

In this chapter, we have modified the variable time-fraction protocol to allow for the use of *CSIT* at the source and relay. For this new set of assumptions, we have provided the modified outage probability. In order to make use of the *CSIT*, we have derived power allocation algorithms which are used at the transmitting nodes. We have developed and studied an optimal *PAA* to minimize the *PEP*. By using the optimal weighting terms for the source and relay, we are able to obtain a coding gain of 3 dB over the basic *PAA*.

To achieve the performance of the *OPAA* we require full knowledge of the *CSIT* at the transmitters. In typical wireless systems, the *CSIT* is fed back from the receiver to

6.3.3 Imperfect *CSIT* and *CSIR*

Having studied the effect of imperfect *CSIT* and perfect *CSIR*, we now examine the more realistic scenario of imperfect *CSIT* and *CSIR*. As discussed earlier in this chapter, the source of *CSI* error in *SPAA* is solely estimation error since we can assume the destination is able to transmit the collaborative transmitter decision without any transmission error. Therefore, with imperfect *CSIT* and *CSIR*, we have that the error at both transmitters and receiver will be the same.

For imperfect *CSIR* we look to the results of Chapter 4. We have the *PEP* given by

$$P_{\Delta_i}(\mathbf{d}, \tilde{\mathbf{G}}) = \mathcal{Q}\left(\sqrt{\gamma_e + \gamma_c}\right), \quad (6.10)$$

where

$$\gamma_e = \frac{E_s}{2\left(N_o + PG_{sd}(1 - \rho_{sd}^2)E_s\right)} 4d_1 \rho_{sd}^2 \left|\tilde{\mathbf{G}}_{sd}\right|^2, \quad (6.11)$$

$$\gamma_c = \frac{E_s}{2\left(N_o + \left(PG_{sd}(1 - \rho_{sd}^2) - PG_{rd}(1 - \rho_{rd}^2)\right)E_s\right)} \text{tr}\left(\tilde{\mathbf{G}}\bar{\rho}\mathbf{A}_c(\mathbf{d})\bar{\rho}^\dagger\tilde{\mathbf{G}}^\dagger\right). \quad (6.12)$$

We note however that in the collaborative phase of the *SPAA* only one transmitter is active. This affects γ_c , since \mathbf{Q} in (4.6) is now either $PG_{sd}(1 - \rho_{sd}^2)$ or $PG_{rd}(1 - \rho_{rd}^2)$, and therefore $(y_{d,t}^c | \mathbf{X}_t^c, \hat{\mathbf{G}})$ is a complex Gaussian random variable with mean either $\sqrt{E_s}\hat{\mathbf{G}}_{sd}\Upsilon_{sd}\mathbf{x}_{s,t}^c$ or $\sqrt{E_s}\hat{\mathbf{G}}_{rd}\Upsilon_{rd}\mathbf{x}_{r,t}^c$ and variance $N_o + \text{tr}(\mathbf{Q})E_s$. Using the same arguments that led to the development of (6.11) ((4.17) in Chapter 4), we can therefore rewrite γ_c as

$$\gamma_c = \begin{cases} \gamma_c^1 = \frac{E_s}{2(N_o + PG_{sd}(1-\rho_{sd}^2)E_s)} 4d_2\rho_{sd}^2 |\tilde{G}_{sd}|^2 & \text{if } |\hat{G}_{sd}| \geq |\hat{G}_{rd}| \\ \gamma_c^2 = \frac{E_s}{2(N_o + PG_{rd}(1-\rho_{rd}^2)E_s)} 4d_2\rho_{rd}^2 |\tilde{G}_{rd}|^2 & \text{if } |\hat{G}_{sd}| < |\hat{G}_{rd}| \end{cases}. \quad (6.13)$$

The *PEP* of the *SPAA* scheme with imperfect *CSIT* and *CSIR* is given by,

$$P_{\Delta}(\mathbf{d}, \tilde{G}_{sd}, \tilde{G}_{rd}) = \begin{cases} Q(\sqrt{\gamma_e + \gamma_c^1}) & \text{if } |\hat{G}_{sd}| \geq |\hat{G}_{rd}|. \\ Q(\sqrt{\gamma_e + \gamma_c^2}) & \text{if } |\hat{G}_{sd}| < |\hat{G}_{rd}| \end{cases}. \quad (6.14)$$

Using $\tilde{G}_{ij} = \sqrt{\zeta_{ij}} \hat{G}_{ij}$ we rewrite (6.14) as

$$P_{\Delta}(\mathbf{d}, \tilde{G}_{sd}, \tilde{G}_{rd}) = \begin{cases} Q(\sqrt{\gamma_e + \gamma_c^1}) & \text{if } \frac{|\tilde{G}_{sd}|}{\sqrt{\zeta_{sd}}} \geq \frac{|\tilde{G}_{rd}|}{\sqrt{\zeta_{rd}}} \\ Q(\sqrt{\gamma_e + \gamma_c^2}) & \text{if } \frac{|\tilde{G}_{sd}|}{\sqrt{\zeta_{sd}}} < \frac{|\tilde{G}_{rd}|}{\sqrt{\zeta_{rd}}} \end{cases}. \quad (6.15)$$

We can now solve for the *FER* of (3.39) by integrating over all \tilde{G}_{sd} and \tilde{G}_{rd} .

6.4 Results

The results presented in this section use the same variable time-fraction collaborative channel code as in Chapter 5.

In Fig. 6.1, we show the performance of the *SPAA* when affected by imperfect *CSIT* and perfect *CSIR*. The results show a significant loss of performance due to imperfect *CSIT*. Even at high *TSNR* we see that there is a significant effect to the *FER*

$$\text{coding gain} \approx \frac{\delta n_p \alpha}{\delta n_p + 1}, \quad (6.16)$$

where we use $\alpha = \frac{n}{n + 2n_p \delta}$, which does not depend on the time-fraction, since the transmitted signal power in the *SPAA* remains constant regardless of collaborative mode. Note also that we use for coding gain the γ_e^{gain} , since for *SPAA* only one node is ever transmitting at any given moment. Therefore the coding gain of the system with imperfect *CSIT* and *CSIR* at high *TSNR* is given by

$$\text{coding gain} \approx \frac{\delta n_p}{\delta n_p + 1} \frac{n}{n + 2\delta n_p}. \quad (6.17)$$

Using the same methods as in Chapter 4, we see that the optimal number of pilot symbols is given by

$$n_p^{opt} = \sqrt{\frac{n}{2\delta^2}}, \quad (6.18)$$

which in our case is about 14 (for $n = 390$ and $\delta = 1$). Furthermore, the optimal number of pilot symbols is never dependent on the relay location, since the different modes of operation all lead to the same coding gain. This is because only one node is ever transmitting at any given moment and the total transmission power is always constant in the *SPAA* protocol.

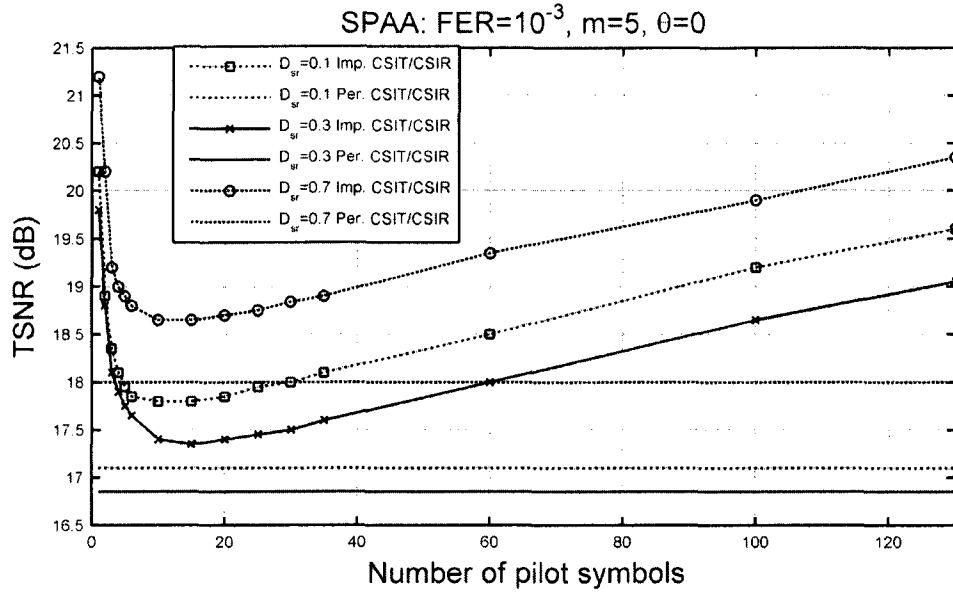


Figure 6.4. Effect of the number of pilot symbols on the performance of *SPAA* with imperfect *CSIT* and *CSIR*.

Lastly, we show in Fig. 6.5 the performance of the *SPAA* protocol with imperfect *CSIT* and *CSIR* for any relay location when using the optimal number of pilot symbols. We see that the coding loss remains constant regardless of the relay's location.

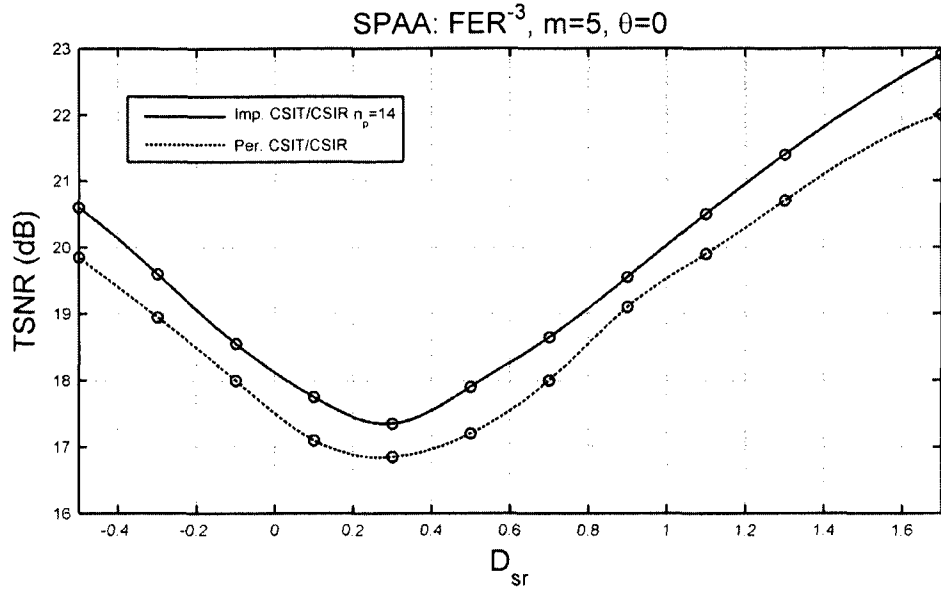


Figure 6.5. Required $TSNR$ to achieve $FER=10^{-3}$ for $SPAA$ with source at the origin, destination at 1 and $\theta = 0$.

6.5 Conclusion

In this chapter we have presented an analysis of the effect of imperfect $CSIT$ on the performance of the $SPAA$ protocol. We have provided a discussion on the source of errors when using the $SPAA$ protocol. It is shown that the best estimation strategy is to have the destination make the estimate and the decision on the transmitter in the collaborative phase.

We have obtained analytical results on the effect of imperfect $CSIT$ on the PEP at the destination for the cases of imperfect $CSIT$ and perfect $CSIR$ as well as imperfect $CSIT$ and $CSIR$. The results show that for any combination of perfect or imperfect $CSIT$ and $CSIR$, we always attain full spatial diversity. The results also show the effect of the

relay location on the optimal number of pilot symbols for the imperfect *CSIT* and perfect *CSIR* scenario. On the other hand, we have solved analytically for the optimal number of pilot symbols when we have imperfect *CSIT* and *CSIR*. For this *CSI* assumption, we have shown that the relay's location does not affect the optimal number of pilot symbols. Our results show that when using the optimal number of pilot symbols with imperfect *CSIT* and *CSIR*, the performance approaches that of perfect estimation to within 0.8 dB at $FER=10^{-3}$ for any relay location.

have multiple receive antennas. We could therefore use decoding methods similar to [83]. In essence, we would decode the signal from one node and treat the other as interference, then remove the decoded signal from the received signal and then proceed to decode the remaining signal. Using soft decoded outputs we could then use the two decoded signals as inputs to a Viterbi decoder. We believe we could still attain a spatial diversity order of 2 using this method.

- In this thesis we have assumed the source has only one relaying node with which it may collaborate. In reality there may be an abundance of possible relays. We may wish to study the optimal relay assignment for the over-all performance of the network. This can lead to a study of fairness of relay assignment. For example, in power constrained scenarios such as sensor networks, we may not wish to use the best relay at all times, given that that relay may be over-used. In order to determine the performance of the *OPAA* or *SPAA* when the source has access to multiple relays, we must extend the feedback requirements. For the *OPAA*, at the end of each time-fraction, the source as well as the available relays must recalculate their optimal weighting terms. On the other hand, for the *SPAA*, at the end of each time-fraction, the source as well as the available relays must determine which node has the strongest channel to the destination. We note that in both those cases, the subset of relays available at each time-fraction changes and must now be determined by an *SNR* metric which includes the source and/or the relays that have been transmitting from the previous time-fractions. As a final comment on the multiple-relay scenario, we also note that new methods to display

results are required. To demonstrate results such as those in Fig. 3.7 would now require multiple dimensions to account for all the relay locations.

- Another research avenue to consider is multi-user collaborative communications. We may consider each source-relay-destination group as one link. From this we may wish to determine the effect of interference. For example, is an increase in collaboration detrimental due to the associated increase in interference? Preliminary results have shown that for low total power, collaboration always shows benefits even in high interference scenarios. On the other hand, for high total power, collaboration does not seem to provide much benefit.

7.2. List of Publications

The following is a list of publications that are based on the results presented in this thesis.

1. P. Toher, H. Khoshnevis and M. R. Soleymani, "Design of collaborative codes achieving space-time diversity," *Proceedures of IEEE International Conference on Communications (ICC) 2007*, Glasgow, UK, June 2007.
2. P. Toher and M. R. Soleymani, "Performance of variable time-fraction collaborative communication," *Proceedures of IEEE Personal, Indoor and Mobile Radio Communications Conference (PIMRC) 2008*, Cannes, France, September 2008.
3. P. Toher and M. R. Soleymani, "Power allocation for wireless communications using variable time-fraction collaboration," *Proceedures of IEEE International Conference on Communications (ICC) 2009*, Dresden, Germany, June 2009.